ADDIS ABABA UNIVERSITY
ADDIS ABABA INSTITUTE OF TECHNOLOGY
SCHOOL OF MECHANICAL AND INDUSTRIAL ENGINEERING

FATIGUE LIFE INVESTIGATION FOR AISI-H13 USED FOR THE APPLICATION OF PICKAXE DIE USING NUMERICAL AND ANALYTICAL METHOD

By: Belay Ayalew

A thesis submitted to Addis Ababa University post graduate office in partial fulfillment of the requirements for the degree of Master of Science in Mechanical Engineering (Mechanical Design)

April, 2023

ADDIS ABABA UNIVERSITY
ADDIS ABABA INSTITUTE OF TECHNOLOGY
SCHOOL OF MECHANICAL AND INDUSTRIAL ENGINEERING

MSc thesis titled

FATIGUE LIFE INVESTIGATION FOR AISI-H13 USED FOR THE APPLICATION OF PICKAXE DIE USING NUMERICAL AND ANALYTICAL METHOD

By

Belay Ayalew

Approved by Board of Examiners:

_____	_____	_____
Examiner	Signature	Date
_____	_____	_____
Examiner	Signature	Date
Dr. Haileleoul Sahle	_____	_____
Chair of Design Stream	Signature	Date

Endorsed By:

Dr. Araya Abera	_____	_____
Dean of the School of Mechanical and Industrial Engineering	Signature	Date

DECLARATION

I, Belay Ayalew, declare that this thesis entitled **"FATIGUE LIFE INVESTIGATION FOR AISI-H13 USED FOR THE APPLICATION OF PICKAXE DIE USING NUMERICAL AND ANALYTICAL METHOD**" is the result of my own research carried out under the supervision of Dr. Haileleoul Sahle. It has not been presented in any from in any other university and all sources of material used for this thesis are accordingly sited and acknowledged. It is submitted in partial fulfillment of the requirements for the degree of Masters of Science in Mechanical Engineering, Mechanical Design at Addis Ababa University.

Belay Ayalew	_____	_____
Student's Name	Signature	Date
Dr. Haileleoul Sahle	_____	_____
Advisor	Signature	Date

ACKNOWLEDGEMT

This MSc thesis is the result of research performed at the School of Mechanical and Industrial Engineering, Addis Ababa Institute of Technology, Addis Ababa University. I would like to acknowledge and express my special thanks of gratitude to my advisor, Dr. Haileleoul Sahle, for giving me the golden opportunity to work on thesis in title ***Fatigue Life Investigation for AISI-H13 used for the Application of Pickaxe Die using Numerical and Analytical Method*****.** He taught me the methodology to carry out the research and how to present the research work clearly. It was a great privilege and honor to work and study under his guidance. I would also like to thank him for his understanding, kindness, patience and our dynamic discussions that brought the research forward. Thank you for always pushing me for more.

Besides my advisor, I would like to thank my thesis committee members for their insightful comments and suggestions, hard questions, and giving me a chance to explain my idea freely to the end.

I am also grateful to Kotebe Metals and Tools industry for allowing me to use all the material and geometrical data of the die and work piece as well as technical data related to the hot forging process and forging machine.

I would like to forward my deepest gratitude to my classmates and friends Natnael Fantaye, Sisay Kebede, and Tariku Debede for their great contribution and support in completing this work. I am sincerely thankful to all the people who have contributed to my work in one way or another.

Words cannot express my gratitude to my caring, loving and supportive wife Rekik and my lovable little son Tewodros who served as my inspiration. I would say thank you.

CONTENTS

LIST OF FIGURES

LIST OF TABLES

LIST OF ABBREVIATIONS

FEM	Finite Element Method
FEM	Finite Element Analysis
ANOVA	Analysis of Variance
HCF	High Cycle Fatigue
LCF	Low Cycle Fatigue
DOE	Design of Experiment
LEFM	Linear Elastic Fracture Mechanics
SIF	Stress Intensity Factor
AISI	American Iron and Steel Institute
HCR	Rockwell Hardness
BH	Brinell hardness
VH	Vickers hardness
Th	Hardening Temperature
Tt	Tempering temperature
S/N	Signal to Noise ratio
DF	Degree of Freedom
SS	Sum of Squares
MS	Mean of Squares

ABSTRACT

The main objective of this research was to obtain optimum forging load and temperature to investigate the fatigue life for the pickaxe piercing die made of AISI-H13 which was working under hot forging process in Kotebe Metal Tools Factory. The die supported to manufacture a pickaxe with circular whole diameter of 52mm. Under estimation of the optimum forging load, the temperature of the pickaxe piercing die, the temperature of die and work-piece, the stoke length of the forging press, press ram speed and coefficient of friction were considered as input parameters. This research approach combined analytical and numerical analysis to find a solution to set target (for estimating the forging load). The geometrical model of the dies and work-piece have been modelled using geometrical modelling software (SOLID WORK) and simulated using numerical simulation software(DEFORM-3D),wchich was adopted to simulate the forging processes using the input parameters. Then, the fatigue life of the lower die was analyzed using ANSYS software. To optimize the forging process parameters (dies and work-piece temperatures as well as coefficient of friction), the Taguchi optimization technique based on analysis of variance (ANOVA) and Analysis of mean value (ANOM) was applied. The forging process parameters were considered as experimental factors and the optimization of the forging load was considered as experimental objective. In order to obtain optimum forging load, the forging process parameters are examined using a three-level full factorial design of experiments and analyzed using MINITAB software. As an output ,the obtimum forging load,working temperature and coefficient of friction were identified with values of 2.16MN,1050C, and 0.3 respectively. Among the three forging process parameters,workpiece temperature is the most significant parameter followed by coeffiecent of friction and die temperature to get the lower required forging load.Their percentage contribution to the forging load was 61.33,37.12, and 0.87% respectively. The results of the simulation and the mathematical model were compared for validation and the identified results agreed with each other. By implementing the minimum optimized forging load(2.16 MN), the fatigue life of the lower pickaxe piercing die can be extended to 10^6 cycles until the die fracture.

Keywords: forging parameters, forging load, optimization process, fatigue life, pickaxe die

CHAPTER1: INTRODUCTION

1.1 Background

Forging is a deformation process in which high compressive forces are applied to a metal (work-piece) above the yield strength in two dies, resulting in plastic deformation of the work-piece. Forging is an important metal forming process, because the parts from the forging process have better mechanical properties than other manufacturing processes. This process refines the grain structure of the metal, removes any gas pockets or voids, improves chemical segregation, mechanical and physical properties, thereby increasing reliability and consistency. In general, the forging process can be classified according to the forging temperature (hot, warm, cold), forging machines (hammer, press), and forging dies (open die, impression die, and flash less die). Hot forging is done at temperatures above the recrystallization temperatures, typically 0.6Tm, or above, where Tm is the melting temperature of the work-piece. During hot forging, lower loads are required because the flow stress gets reduced at higher temperatures[1, 2].

Dies and tools used in the hot metal forming (extrusion, forging, rolling, etc.) are exposed to high pressures (forces), elevated temperatures, and mechanical and thermal fatigue. The three main modes of die failure in-service are fatigue (brittle failure caused by crack propagation), wear (gradual wearing out of the bearing surface), and deflection (plastic deformation). Fatigue failure starts with the development of fatigue cracks, the propagation of which ultimately leads to the inability to produce quality products. The concentrated and cyclical stress and brittle failures are generally located at a cross-sectional change, a sharp corner, stamp mark, etc. Large cyclic stresses combined with regions of high stress concentration in cavities leads to the formation (initiation), growth and propagation of cracks[3]. The friction between the billet and the die land results in wear and surface tear. Thus, the accumulated wear can lead to die failure. In forging processes, the preheating of the die and billet (work-piece), a high forging pressure in the die and the unbalance forces between the die and the billet can lead to deformation or deflection of the die. These deformations and deflections could also lead to die failure. Among the three common die failure modes, approximately 46% of die failures are fatigue fracture, 26% are wear, 9% are deformation or deflection, and the rest are the miscellaneous failure modes. Out of these three, fatigue fracture is the principal cause of failure[4]. Fracture mechanics methods are used to investigated the three stages of fatigue life, crack initiation, crack propagation and final fracture.

Therefore, in order to determine the safe service life, the investigation of fatigue life due to cyclic load, loading is an important design criterion.

The finite element method (FEM) is the most commonly used numerical technique in the hot forging process and is carried out at different forging temperatures to study the effect on the effective stress of the die material. The results of the FEM analysis show that the effective stress decreases as the initial temperature of the work-piece increases. The most common analytical methods used to estimate the forging loads are slip-line, slap-line, and upper bound. The predicted pressure distribution and forging forces are used to compare the methods for a number of forming conditions. By minimizing the forging load, the stress induced in the die was reduced and the life of the die was increased. Process parameters (factors) such as work-piece temperature, die temperature, friction coefficient, and die speed affect the forging process, which must be appropriately controlled or monitored during the forming process. To validate the model, verification is required by comparing some parameters from measured experimental tests with the values of some parameters obtained by simulation software.

1.2 Statement of the problem

The hot forging die is critical part of the hot forging process. Due to the variation in forging load, the die fails due to fatigue. The die used in the hot forming of metals is exposed to high pressures, elevated temperatures and mechanical and thermal fatigue load. Due to the involvement of multi-forging process parameters in the hot forging operation, users face the challenge of controlling (monitoring) the process parameters in the forging process. Because of this problem, the die was overstressed (overloaded) by fluctuations (variation) in the forging load and exposed to mechanical fatigue loading, resulting in premature failure of the die. Therefore, the cost for the user due to the replacement of defective die materials and production downtime are high. In order to reduce the cost of failed die material, maintenance costs, production downtime costs and to extend the service life (fatigue life) of the forging die, maintaining optimal forging load and forging temperature is the critical concern required. Controlling (monitoring) the forging process parameters in terms of the properties of the die material as well as optimizing the forging load and forging temperature is the first task for the next fatigue life investigation of the pickaxe piercing die. by using optimized forging load and temperature in the forging operation, accurate die life prediction can be achieved.

1.3 Objective of the Study

1.3.1 General Objective

The objective of this research is to obtain optimum forging load and temperature to investigate the fatigue life for AISI-H13-die material used for the application of pickaxe piercing die adopting numerical simulation.

1.3.2 Specific Objectives

- To identify the forging process parameters and their effect on the die fatigue life.
- To investigate the effect of forging process parameters on the forging operation.
- To model the forging process by using finite element modeling (FEM) software.
- To predict (estimate) the forging load using analytical and numerical methods, optimize and validate the results with each other.

1.4 Limitations and Scope of the Study

This study investigates the fatigue life of pickaxe piercing die which was working under elevated forging temperature in the hot forging industry. Two methods of theoretical analysis are employed in this problem: the finite element method (FEM) and analytical methods (Slip-Line and slab-line Methods). For economic reasons, the experimental test (laboratory test) for the pickaxe piercing die was not performed. For the analysis of the forging process and fatigue life of the die, the finite element method was adopted using the commercial software DEFORM-3D and ANSYS, respectively. Due to the involvement of multi-parameters in the forging process, the pickaxe piercing die is venerable for different types of failures such as mechanical and thermal fatigue, wear, and plastic deformation. This study focuses only on mechanical fatigue and does not consider thermal fatigue, wear, and deformation. The exclusion of these failure analyses represents a limitation of the study.

1.5 Organization of the Study

The entire thesis contains six chapters in addition to appendices and references. Chapter one outlines the background of forging and the main objective of the project, as well as the specific objectives of this research and the overall perspective of the document. Chapter two gives a

literature review on forging and the failure mechanisms of forging dies. Chapter three describes the material, method and conditions. Chapter four discusses the analytical methods approach. Chapter five discusses the results of the experiment and the validation of the data. Chapter six represents conclusions and future recommendations.

CHAPTER2: LITERATURE REVIEW

2.1 Introduction

This chapter covers the overview of different research works related to metal forging processes, potential failures encountered in the hot forging process and previous related research work to the selected research topics. Hence, the review is organized based on mathematical and numerical modeling techniques of the forging process and effects of process parameters in die life.

2.2 Previous Related Work

2.2.1 Based on Effect of Stress and Fatigue Life of Dies

Sam Josh et al. [5] investigated the impact of the initial die temperature on the effective stress of the die material by performing a Finite Element Analysis using DEFORM 3D simulation software at various die temperatures ranging from 150°C to 350°C. The result showed that the effective stress of the die decreases as the initial temperature of the work piece increases. Ayer[6] used numerical analysis techniques to study the AZ31 magnesium helical gear forming process. Temperature change, effective stress, effective strain, and forming load were all calculated using a 3D finite element analysis. B.A. BEHRENS and T. HADIFI[7] conducted thermomechanical fatigue tests to simulate loading conditions in the die cavity, which was the location where the highest mechanical load and temperature are found at the same time. The experimental tests were conducted to understand the fatigue behavior of the steel and to provide test data for FEA-based simulations. To reproduce the material's behavior in the tests, a Chaboche-type material model available in the nonlinear FEA solver LS-DYNA is used. Based on this approach, a very good agreement between simulation and experiment was achieved. Olivier Brucelle and Gérard Bernhart [8] describe the methodological approach used to investigate the reasons for cracking and propose a solution to increase service life. They used a combined numerical and experimental approach. Their work clearly shows the advantages of a methodology based on combined numerical and experimental approaches to determine the thermomechanical stress field in hot forging tools in order to derive solutions for extending the service life. Bernd-Arno Behrens et al.[9] investigated the effect of different radii on the lower die of the forming tools. It was found that a larger radius leads to a reduction in stresses, and they conclude that their results

will be used in further research to calculate tool life under thermomechanical cycling. Johng-jokim and chang-hyok choi [10] investigated the life of the forging die based on the fatigue life and the amount of wear, which were considered to estimate the die life. The main objective was to develop the equations to adapt finite element analysis to life estimation for a hot forging die. The Archard's model was used to estimate the wear life of the die, and the Goodman's and Gerber's equations were applied using the stress-life method to estimate the fatigue life. Gh. Seyed Bagheri et al.[11] studied the hot forging process of a spline hub and were simulated using the finite volume method to investigate the applied stress states of the forging die. The influence of controllable parameters (e.g., - forging temperature and flash thickness) on fatigue life was also investigated. The Results show that increasing the forging temperature and flash thickness both lead to an increase in fatigue life. Shravan Kumar and ChakradharGoud S [12] Analyzed the lower die using ANSYS software to identify the stress areas and examined the damage to the D6 material in critical areas. In the beginning, a load application model was used in numerical simulation. Using the model, a crack and failure analysis of the die was carried out, and the optimum arrangement of the cracked die during heat treatment and non-heat treatment was determined. Deformation, principal stresses, stress intensity, and equivalent stresses are just a few of the variables they consider when creating impact analyses. A static impact load was found to cause variations in the cracking tool's stress. Erik Calvo-García et al. [13] examined the axial fatigue behavior of two H13 hot forging tool steels at room temperature within the HCF domain. The Two steels that met the same H13 specifications were used for the fatigue tests. For comparative purposes, stress values leading to the HCF domain under normal conditions were used in these fatigue tests, which were also performed on specimens in contact with a corrosive medium. 10 Hz sine waveforms with a stress ratio of zero were used to load-control all of the tests. Before the fatigue tests, a microstructural analysis was conducted. The corrosion fatigue lives of the H13 steels were found to be significantly lower than the fatigue lives obtained under normal conditions, as demonstrated by the fatigue test results. Furthermore, a reduction in fatigue life was observed even when the test stress range was reduced. The mechanical damage resulting from applied stress was significantly greater than the corrosion damage at higher stress levels. As a result, it was discovered that the fatigue life was constant irrespective of the testing environment. Microstructural and surface defects were the cause of the cracking in the normal tests of the microstructural analysis, whereas corrosion pit formation was the cause of the

cracking in the corrosion fatigue tests. Furthermore, a fracture surface analysis showed that different crack propagation areas were seen in the two steels. The fracture surface analysis suggested that the two steels had different levels of fracture toughness.

2.2.2 Based on Forging Process Parameters and Optimization

Japeth Oirere Obiko et al.[14] carried out research on utilizing the Taguchi method and Deform-3D simulation software to optimize the forging process for X20 boiler pipe steel. The analysis was conducted using three forging factors: the coefficient of friction, die speed, and cylinder temperature. The results showed that the forging parameters have a significant difference with the responses (forging load and maximum tensile stress). Om Prakash Kumar and Vivek Kumar[15] optimized pitman arm forging parameters by modifying the design and process parameters with the aid of simulation software based on finite elements (Deform 3D). Effective and efficient optimization was achieved with the aid of the simulation software. The forging load was used as the objective function of the study, and Taguchi design was used to analyze the data in order to get the optimal results. The optimal values for the work-piece temperature, the die temperature, the coefficient of friction, the damage, and the flash thickness were all determined using the optimal forging load. Kumar Satyam et al. [16] investigated the effect of design and process parameters on forging die load. The FEM based simulation software package DEFORM 3D V6.1 was used to simulate the hot forging process for connecting rod. Four parameters, namely flash thickness, billet temperature, friction coefficient, and corner radii, were found to be the most significant parameters affecting the forging die load under a confidence level of 95%. Rajkumar Ohdar et al. [17] used 3D finite element analysis DEFORM 3D Software with Taguchi method to simulate the closed die forging process for automobile spring saddle. Series of optimization iterations were performed to achieve optimal level of process parameters. Flash thickness, billet temperature and friction coefficient were considered as the most significant parameters affecting the response. Turki Diwan Hussein et al. [18] used the finite element software ABAQUS to analysis and simulate the deformation process. The main objective of the work was to develop a new design and create a virtual experimental model to minimize the generation stresses in hot forged products by controlling some parameters and variables. Akshay S Nandalgaonkar and Sachin C Borse[19] studied the metal forming behavior during closed die forging of an automotive driveline component (Yoke). The Forging process was simulated in the

SIMUFACT Software. The effect of selected forging parameters on the forging load and effective stress is determined. It was found that the billet temperature, die temperature, flash thickness and friction have a significant effect on the forging load. Among the four parameters, the temperature of the billet was the most significant parameter followed by the flash thickness and the friction factor (in that order). M. Jolgaf et al. [20] conducted a numerical simulation for the closed die forging process of AlMgSi matrix with 15% Sic particles was simulated with ANSYS software to investigate the material flow behavior and predict the forging load and strain distribution. The forging process was optimized using the ANSYS optimization module.

2.2.3 Based on Forging Force Estimation Methods

Maryam saleh[21] conducted a study on forging process of the tools (dies), analyzing the forging problems with analytical methods (upper bound approach) and comparing the results with simulation and experimental results. The analytical result agreed well with software simulations and experimental findings. D.Sheth et al. [22] used both theoretical (analytical) modeling and LS-DYNA modeling in order to facilitate the FEM analysis for forging load determination. In order to predict the forging load on the lead for a typical axisymmetric upsetting operation with inclined surfaces, theoretical estimation was conducted using the slab method. Using the LS-DYNA software, a simulated model was created and the results from the theoretical estimates were compared. The accuracy was verified by the forming loads calculated from FEA using LS-DYNA, which were found to be fairly close to the experimental results with percentage errors within 6%. Forging load estimates in theoretical values were slightly higher than in experimental observations. Ayer23] used a combination of the upper bound method (UBM), neural network model (NNM), and finite element method model (DEFORM-3D software) to simulate and predict the deformation load in bimetallic materials that are upsetting. Without the need for experiments, the suggested ANN, FEM, and UB models predict the forming load and offer insightful information about the parameters influencing the forming load.

2.3 Effect of Forging Parameters on Die Life

2.3.1 Forging Temperature

Temperature is an important factor (parameter) in metal forming because the properties of a metal change as the temperature increases. Therefore, the metal responds differently to the same

manufacturing process when it is performed at different temperature. At low temperatures, good surface finish, strength and hardness, and closed tolerance can be achieved during forging, but the amount of stress required to deform the metal is higher. As temperatures increase, deformation becomes easier, ductility increases, and the metal's grain structure is refined resulting in better physical properties. In addition to the lower flow stress, the service life of work tools also reduced at higher temperatures. Because lubrication is more difficult, the work metal tends to oxidize, abrasive scales appear, and poor surface finish result from the lack of adequate lubrication, oxide scales, and roughened dies. In general, increasing the hot forging temperature reduces the flow stress, the strain hardening coefficient and thus the forging resistance of the material to deformation (the forging load requirement would go down). The plastic deformation and friction generate additional heat during the forging process. A fraction of the mechanical energy generated during the forging process is converted into heat. This can contribute to an increase in forging temperature if the strain rate is reasonably high. The temperature distribution and magnitudes in metal forming are primarily affected by the initial temperatures of the workpiece and die, heat generation at the work-piece-die interface from plastic deformation and friction, heat transfer between the workpiece and dies, and heat transfer between the workpiece and the environment (coolant, air, lubricant, etc.)[23]. The average instantaneous temperature in the deforming work-piece can be estimated by:

$$T_{avg} = T_W + T_D + T_F - T_{con} + T_{rad} + T_{cov} \qquad [2.1]$$

Where, Tw= the initial work-piece temperature

T_D= the temperature increases due to plastic deformation

T_F = the temperature increases due to interface friction

T_{con}= the temperature drops due to heat transfer into the dies by conduction

T_{cov}= the temperature drop due to convectionto the environment

T_{rad}= the temperature drop due to radiation to the environment

2.3.2 Die Temperature

Preheated dies are generally used in the hot forging process to avoid thermal stress effect at die and work piece interface which reduces the metal flow at surfaces. The heated dies also facilitate die filling and reduce forging pressures. Forging work-piece cooled very rapidly if dies are not

heated due to conduction between forging work-piece and the dies. From the rule of conservation of energy as shown in following formula;

$$Q = q_{con} + q_{rad} + q_{cov} \qquad [2.2]$$

Where Q=total heat loss

q_{con}= heat losing by conduction

q_{rad}= heat losing by radiation

q_{conv}= heat losing by convection

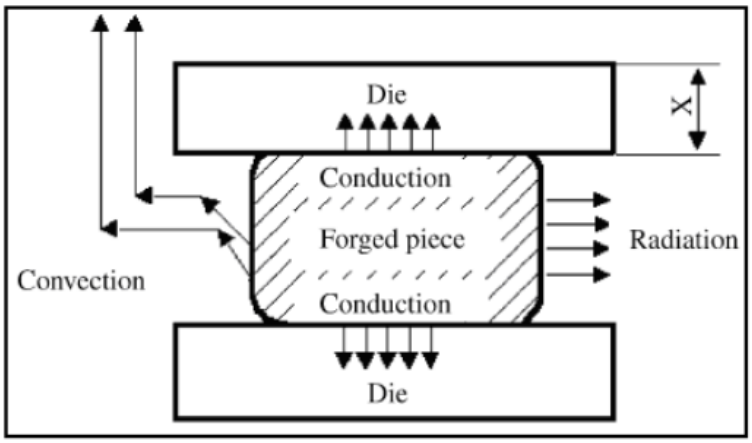

Figure 2. 1: Cooling of forging work piece

Table 2. 1: Die Temperature Ranges for Different Forging Equipment

Forging Equipment	Die Temperature Range (^{O}C)
Mechanical Presses	150-260
Hammers	95-150
Hydraulic Presses	315-430
Roll Forging	95-205

2.3.3 Friction

Metal forming process involves larger forces for deformation and hence high pressure exists between the contact surfaces of the die and the work metal. Since, friction is the resistance to sliding along an interface, the higher the contact pressures, the higher will be the friction resulting in an increase in the deformation resistance of the work metal. The frictional resistance is due to the surface asperities that are present at the micro- scale on both the dies and the work piece[24]. Friction increases the amount of force or power required to perform an operation.

Friction dissipates energy and increases the force required to deform a material because it generates heat and hence increases the force needed to deform a material. The generated heat complicates the control of the deformation temperature. It can affect the material flow during deformation and leads to inhomogeneous deformation[16].

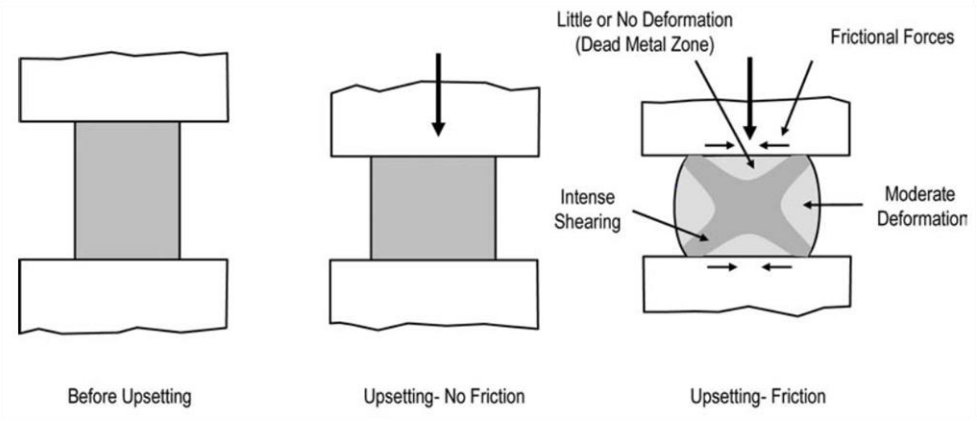

Figure 2. 2: Schematic diagram for friction effect for forging die [44]

2.3.3.1 Modeling of the Effects of Friction on Forging Process

The coefficient of friction (μ) during a forging operation plays an important role in the plastic deformation behavior of metals when they deform with large deformation during manufacturing processes. The coefficient of friction is a system property rather than a material property because it depends on the work-piece material, the die material, and a lubricant[25].

Model one: The first model is referred to as Coulomb's law. The frictional stress component is directly proportional to the pressure that exists between the die and the work piece at the point of interest. The value of μ can vary between 0 and $1/\sqrt{3}$ (i.e., 0.577). At low pressure, this equation is a good description of the frictional stress component. Using coulomb's friction law

$$\mu = \frac{\tau}{P} \Rightarrow \tau = \mu * P \qquad [2.3]$$

Model two: The second model is called the constant friction factor equation. It is assumed that the frictional stress component represents a fraction of the flow strength $(\sigma_o)$of the work piece. This can be better described at higher pressures at the interface.

$$\tau = m\frac{\sigma_o}{\sqrt{3}} \qquad [2.4]$$

2.3.4 Lubrication

In order to avoid metal-to-metal contact, lubricants are used. Lubricants used in the manufacturing industry for metal forming processes included vegetable and mineral oil, soaps, graphite dispersed in grease, water-based solutions, solid polymers, wax, and molten glass. Oil-based lubricants can cause excessive wear (erosion) due to the explosion-like combustion of oil between the billet and the cavity[26]. On the other hand, water base lubricants cool the die surface to a greater extent, increasing the risk of cracks due to thermal fatigue.

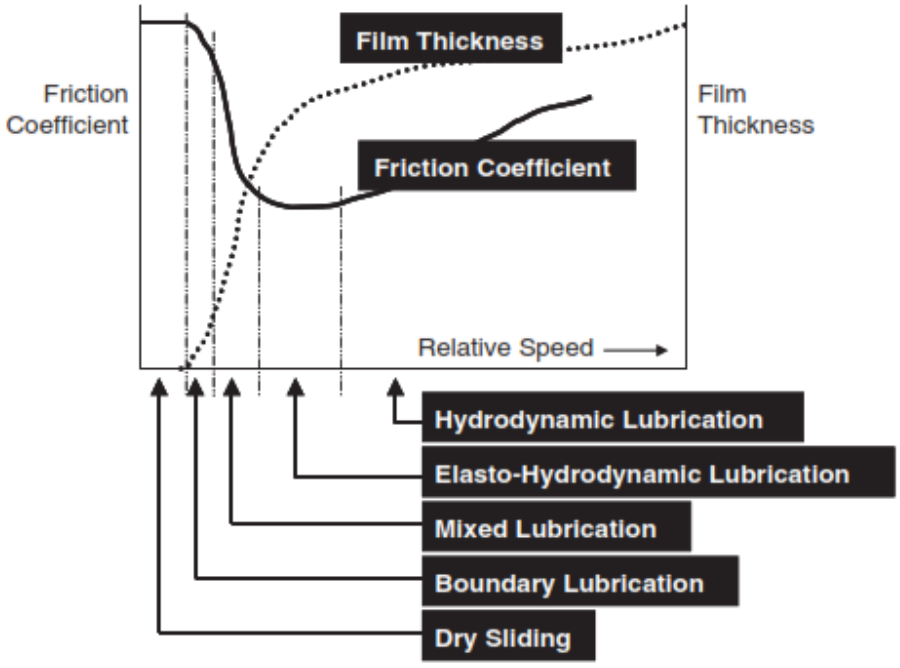

Figure 2.3: Stribeck -curve-Different frictional regimes in forming operations[24]

2.3.5 Flow Stress of Metals

Flow stress is the instantaneous stress value that is required for continuous deformation of the material. Factors (parameters) related to the deformation process are deformation temperatures (T), degree of deformation or strain (ε), and rate of deformation or strain rate ($\dot{\varepsilon}$). Therefore, the flow stress (σ_o) can be expressed as a function of temperature (T), strain (ε) and strain rate($\dot{\varepsilon}$):

$$\sigma_o = f(T, \varepsilon, \dot{\varepsilon}) \qquad [2.5]$$

In hot forging of metals at temperatures above the recrystallization temperature, the influence of strain rate (i.e., rate of deformation) becomes increasingly important. In cold forming), the effect of strain rate upon flow stress is negligible, and the effect of strain (i.e., strain hardening) on the flow stress is the most important. At a given temperature, it is possible to approximate the variation of flow stress (σ_o) as a function of strain rate ($\dot{\varepsilon}$) by:

$$\sigma_o = C\dot{\varepsilon}^m \qquad [2.6]$$

The constant C, indicated by the intersection of each plot with the vertical dashed line at strain rate =1.0, decreases with increasing temperature and m (slope of each plot) increases with increasing temperature. As the temperature increases, the strain rate becomes increasingly important in determining flow stress.

Table 2.2: Values of strength constant(C) and strain rate sensitivity (m) for AISI1045

Material-AISI1045	Strain(ε)	Temperature (900 ^{0}C)		Temperature (1000^{0}C)		Temperature (1100^{0}C)		Temperature (1200^{0}C)	
		m	C(Mpa)	m	C(MPa)	m	C(MPa)	m	C(MPa)
	0.05	0.080	175	0.089	104	0.100	77.2	0.175	55
	0.10	0.082	199	0.103	129.6	0.125	93	0.168	64.8
	0.20	0.086	229.6	0.108	157	0.128	106	0.167	72.4
	0.30	0.083	244	0.110	169.6	0.162	106.8	0.180	74.5
	0.40	0.105	244	0.134	170.3	0.173	108.9	0.188	74.5

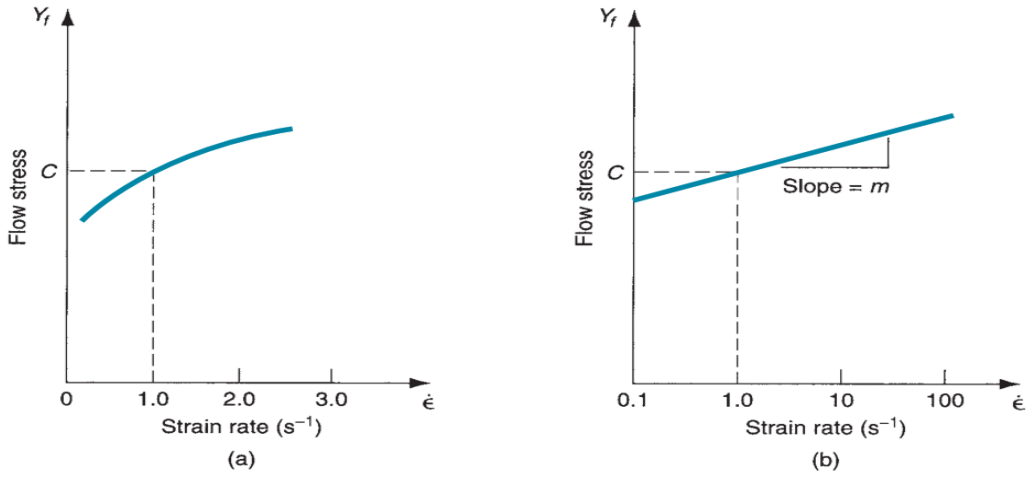

Figure 2.4: Effect of strain rate on flow stress at an elevated work temperature.

2.3.6 Forge Ability of the Material

A metal's forgeability refers to the ability to undergo deformation without causing defects such as discontinuities or cracks. Common tests for forgeability include upsetting and hot-twist. The test is recommended to be performed at similar operating condition as experienced in forging, such as temperature, strain rate. The forgeability also depends on material characteristics such as tendency to grain growth and oxidation. Relative forgeability can be directly used for open die forgings, whereas die filling ease as a function of relative forgeability and flow stress/forging pressure is applicable to closed die forging[24].

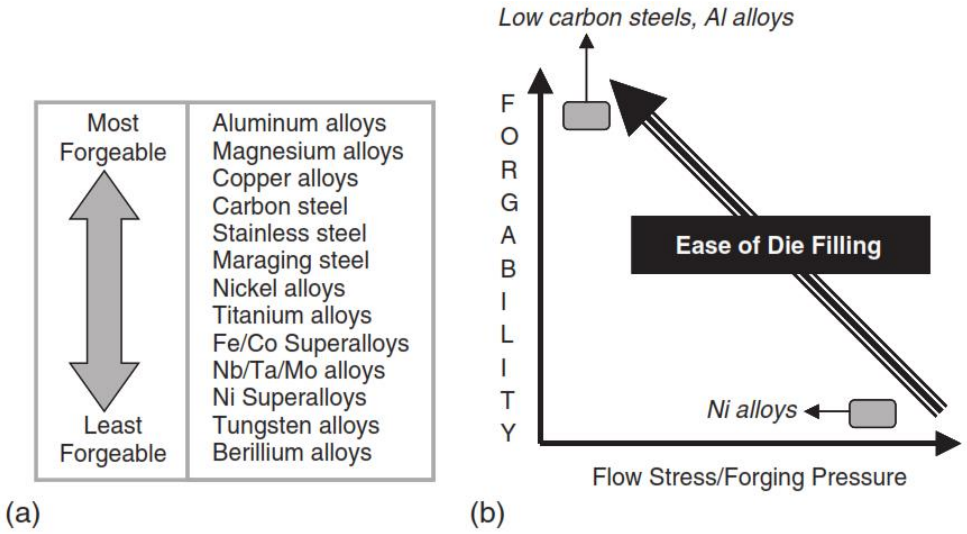

Figure 2.5: (a) Relative forgeability and flow stress/forging pressure[24]

2.3.7 Shape Factor of Component and Die

The metal flow in the die cavity is strongly influenced by the geometry of the component and die. The simple shaped parts are easier to forge, compared to the complex shaped parts. The components with higher surface area per unit volume can called complex shapes for forging. These parts with increased surface area are more critically affected by friction and temperature variation. As a result, the forging load tends to increase to completely fill the die cavity.

2.4 Fundamentals of Plasticity in Metal Forming

In deformation, the internal resistance within the work piece to these external loads applied to the work piece varies from point to point. The measure of this resistance is the internal stress that exists in the work piece. when plastic deformation occurs at a specific point in the work-piece, the internal stress is equal to the flow strength of the material at that point[27].

2.5 Causes of Die Failure

Factors affecting the life span and wear of the die depends on several factors, including die material and hardness, composition of the work-piece metal, forging temperature, condition of the work-piece metal on the forging surfaces, type of equipment used, and work-piece design. The three-main cause of premature die failure are died overload, wear, and overheating[16].

2.5.1 Overloading of the Die

An overloaded die wears out rapidly and can break. Overloading can be avoided by careful selection of die steel and die hardness, use of blocks of sufficient size, proper application of working pressure, proper die design to ensure correct metal flow, and proper seating of dies in the hammer or press[16].

2.5.2 Wear on the Die

Wear is particularly severe if the design of the forging is complex (difficult-to-forge), if the metal being forged has high heat strength, or if there are metal scales on the work-piece metal. Wear cannot be eliminated, but its effects can be minimized through good die design. This also includes a smooth transition of the forging's shape from one die impression to the next, careful selection of die composition and hardness, and a forging technique that includes: proper heating, and necessary descaling, and correct die lubrication[16].

2.5.3 Overheating of the Die

When a die becomes hotter, the resistance to wear is decreased. Overheating causes most of the premature die wear that occurs in forging. Overheating is likely to occur in the areas of the die impression that project into the cavity. Additionally, continued forging can cause overheating. If an internal die cooling system that prevents overheating cannot be economically provided, dies that are vulnerable to overheating should be constructed from steel with high heat resistance.

2.6 Mechanical Fatigue Life Analysis Approaches

There are three major fatigue life methods for estimating fatigue life, each of which is more accurate for some types of loads or materials. The three methods are: the stress-life (total life) method, the strain-life (crack initiation) method and, the fracture mechanics (crack life) method.

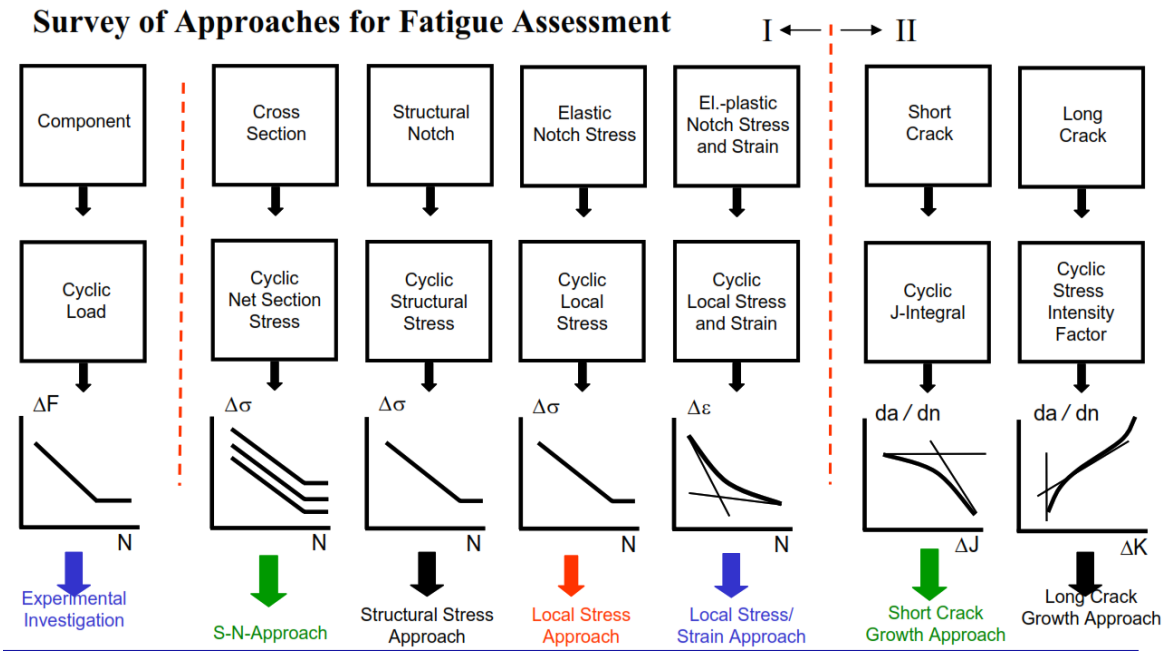

Figure 2.6: Survey of approaches for fatigue assessments

2.6.1 Stress Life Method

Stress Life is concerned with total life(crack initiation plus crack life) and does not distinguish between initiation and propagation. Stress Life is based on S-N curves (Stress – Cycle curves) and has traditionally dealt with relatively high numbers of cycles(greater than 10^5 cycles inclusive of infinite life) and therefore addresses High Cycle Fatigue (HCF)[28]. From the S-N diagram, the die fatigue life can be determined based on the given amplitude and mean stresses.

$$N_f = N_e * \left(\frac{\sigma_a}{S_e}\right)^{1/b} \qquad [2.7]$$

Where, N_e=number of cycles till fatigue limit, N_f=number of cycles till failure, σ_a=stress amplitude, and S_e=Endurance limit. Forging dies are loaded and then completely unloaded, they ideally have ratios of R=0 and A=1, this means that using Gerber or Goodman's equations to deduce the cycles till failure is useless. Therefore, the graphical approach was used and endurance limit was estimated.

2.6.2 Strain Life Method

Strain Life is typically concerned with crack initiation.In terms of cycles, Strain- Life typically deals with a relatively low number of cycles(fewer than 10^5 cycles) and therefore addresses Low Cycle Fatigue (LCF).

2.6.3 Fracture Mechanics (Crack Life) Method

The linear elastic facture mechanics (LEFM) methods assumes that a small crack already exists in the material and calculates the number of loading cycles required for the crack to grow large enough to completely fracture the remaining material. LEFM assumes linear elastic material behavior only. For this to be successful, the plastic zone in front of the crack must be small compared to the crack length[29] This method is more applicable to high cycle fatigue. LEFM usually dominates in brittle materials and the crack growth criterion is described by the stress intensity factor (SIF). There are cases where LEFM does not control (govern) the growth rate of fatigue crack, e.g., such as short crack growth, crack growth in welded areas, low cycle fatigue, crack growth under large scale flow condition (yielding regime), etc. In such cases, the elastic plastic fracture Mechanics (EPFM) parameters J-integral and CTOD can be used as a driving one's force for cracks can be considered[30].

$$\frac{da}{dN} = C(\triangle K)^m \qquad [2.8]$$

where ΔK is the range of the SIF during a fatigue cycle, C and m are the material characteristics, and da/dN is the rate of crack growth.

2.7 Methods of Forging Load Analysis

Analytical methods require a simplification of the problem, but give a quick overall sense of how the processes work and the influence of key process variables (parameters). They also provide simple checks on sophisticated numerical analyses. A primary objective of mathematical analysis of a forging process is to estimate the forging load. Modeling methods that have been used for analyzing metal forming problems include[31]:

2.7.1 Upper Bound Theorem

The upper bound approach based on estimating the external work with the internally energy for deformation. There are two sets of limit theorems: upper bound and lower bound. The lower

bound theorem is not widely used for forming because it underestimates forging loads. The upper bound analysis overestimates the forming load. The upper bound and lower bound limit theorems are the two sets of limits. The actual loads needed are located in the region between the upper and lower limits. Compared to the slip line field approach, limit analysis is practically more accurate and is generally much simpler to apply to a problem.

2.7.2 Slip Line Field Analysis

Slip line field analysis is used to model plastic deformation in plane strain only for a solid that can be represented as a rigid-plastic body. It is more accurate for non-homogeneous deformation (do not assume homogeneous uniform deformation). This method analyses the quite simple problem of the pressure under the indentation of a narrow frictionless punch. It also applied to forming processes such as rolling, strip drawing and slab extrusion. Slip lines are planes of maximum shear oriented at 45 degrees to the axes of principal stresses. Maximum and minimum slip lines are orthogonal. In the slip-line field method, the metal outside the plastic zone and the tools are assumed to be rigid. The rigid material upstream of the plastic zone changes to the plastic state during steady-state forming when it crosses the boundary slip line. Thus, the slip-line field method, like the uniform energy method and the slab method, ignores the effects of elastically loaded material surrounding the plastic zone[32].

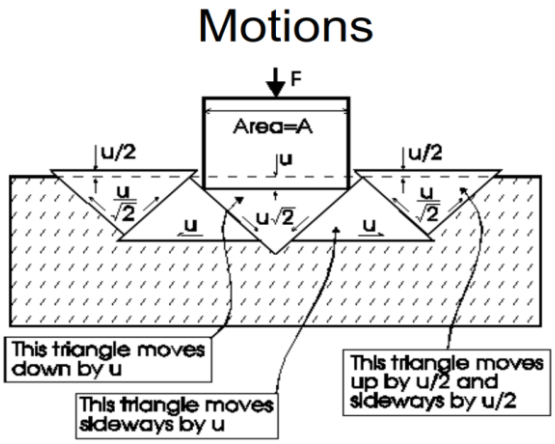

Figure 2.7: Schematic diagram for slip-line analysis

The upper-bound theorem states that the estimate of force obtained by equating internal energy dissipation with external forces is equal to or greater than the correct force.

$$\dot{E} = \dot{W}_{internal} + \dot{W}_{shear} + \dot{W}_{friction} \geq \text{Forming Load} * \text{Velocity of punch}$$

$$\int_V \bar{\sigma}\dot{\varepsilon}dV + \int_{S\Gamma} K|\Delta V|dS + \int_{Sf} mK|\Delta V|dS \geq F * u = \sigma_{avg} * u * A$$

- $\int \bar{\sigma}\dot{\varepsilon}dV$ =the rate of work done due to plastic straining
- $\int k|\Delta V|dS$ =the rate of energy dissipated in internal velocity discontinuity
- $\int mk|\Delta V|dS$ =The power consumed for friction.
- $|\Delta V|$ =The rate of relative slip velocity along surface S.
- $\dot{\varepsilon}$ =the effective strain rate in an element of volume dV
- K= the yield shear stress due to friction along S.
- Sf=the surface over which friction is exerted
- $S\Gamma$=The surface area between the punch-work piece and velocity discontinuity
- m=the friction factor (o for friendless and 1 for sticking friction
- F=the upper-bound load at a forging velocity (velocity of the ram) of u.

Generally, for continuous velocity field the second term can be ignored, $\int k|\Delta V|dS = 0$

$$\dot{E} = \int_V \bar{\sigma}\dot{\varepsilon}dV + \int_{Sf} mK|\Delta V|dS = F * u = \sigma_{avg} * u * A$$

$$\Rightarrow \dot{E} = F * u = \text{Forming Load} * \text{Velocity of punch}$$

$$\dot{E} = F * u = 2K\left(S * \frac{u\sqrt{2}}{\sqrt{2}} + S * u + S * \frac{u}{2} + S * \frac{u}{2}\right) = 6KSu,$$

using $\sigma_{avg} = \frac{F}{A} = P \Rightarrow F = P * A$ and $V = A * u = Su$

$$PAu = 6KSu \Rightarrow PV = 6KV \Rightarrow P = 6K \qquad [2.9]$$

The rate of external work done in the process is equal to internal power required for homogeneous deformation plus rate of work done in shear or redundant deformation plus rate of work done for overcoming friction.

2.7.3 Slab-Line Method Analysis

The slab method is a simple but effective analytical technique for calculating forging loads and stresses. The primary benefit of the slab method is that it allows the division of a complex

forging into some basic deformation units or blocks that can be analyzed separately[33]. The slab method assumes that the metal deforms uniformly in the deformation zone. It is a simple analytical procedure based on principles of mechanics. A simple relationship between forging load and material flow stress in the forge is assumed: F = k A, where k is an empirically determined constant which considers friction, redundant deformation etc. The general methodology involved in slab method can be stated as follows:

1. First the material under deformation is sliced into infinitesimally small portions.
2. Then force balance is made on the small element.
3. From force balance a differential equation in terms of the forming stress, geometric parameters of the billet and friction coefficient is formulated.

This differential equation is solved with suitable boundary conditions. The solution gives the required forming stress. This method may involve some simplifying assumptions. Hence this method may be considered approximate. Moreover, it may not be easy to apply this method for more complex forming processes, such as impression die forging. Slab method is developed with the assumption that the material flow is homogeneous during forming.

- the forging force (F) attains its maximum at the end ot operation.
- The length of the element(dx) is much more than the other two dimenstions so that a condition plane strain exist.
- The work piece material behaves like a ideal plastic material and and the operation is taking place in plastic range.
- The coficient of friction(μ) between the workpiece and the die remain constant.
- The forged material follows the von-mises falure criteria.

The variation of the stress field along the y-direction is negligible and is not considered. Because, the thickness of the work-piece is assumed to be small as compared with its other dimensions, and during the forging process, the entire work-piece will be in the plastic state.

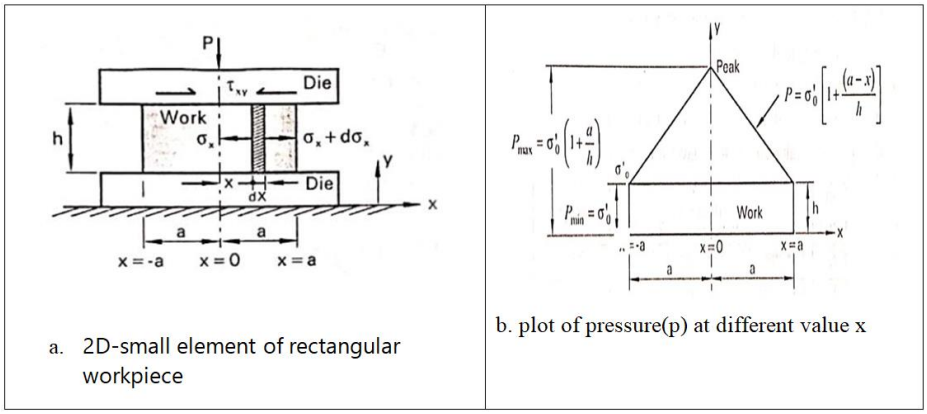

a. 2D-small element of rectangular workpiece

b. plot of pressure(p) at different value x

Figure 2.8: a forging of rectangular work piece and its forging pressure distribution[26]

The stressess acting on the faces of the slab are, P_x –the die pressure, τ_x-the frictional stress at the die-work-piece interface, σ_x and $\sigma_x + d\sigma_x$ are lateral stresses acting on the vertical faces of the slab.An element under the die of length (dx) is subjected to a longitudinal stress (σ_x) and a vertical stress(σ_y) due to a die pressure(p). Since the strip is symetric about the center line,only the slab in the right hand half of the strip is considered.The equilbrium of the forces acting in x-direction is made up of two components.

1. Due to the change in longitudinal stress with x increasing posetively to the left.
2. Due to the die pressure at the two interfaces.

Equilbrium forces in the "X" direction (horizontal).

$$\sum F_x = 0 \Rightarrow (\sigma_x + d\sigma_x) * hb - (\sigma_x) * hb - (2\tau_x) * dxb = 0$$

$$(d\sigma_x) * h = (2\tau_x) * dx \Rightarrow \frac{d\sigma_x}{dx} = \frac{2\tau_x}{h} \qquad [2.10]$$

With coulomb friction, $\tau_x = \mu * P$. Substituting this in equation [26]

$$\frac{d\sigma_x}{dx} = \frac{2\tau_x}{h} \Rightarrow \frac{d\sigma_x}{dx} = \frac{2\mu P}{h} \qquad [2.11]$$

Equilbrium forces in the "y" direction (vertical)

Taking σ_x and P_x as the principal stresses, $\sigma_1 = \sigma_x$, $\sigma_2 = \sigma_y = -P_x$

$$\sum F_y = 0 \Rightarrow \sigma_y * dx + P * dx = 0 \Rightarrow \sigma_y = -P \qquad [2.12]$$

Relating the two principal stresses by means of the yield criteria for plane-strain conditions, the von-mises and tresca criteria are equevalent. In the case of stiking friction,the frictional stress on the die and the workpiece interface is equal to k(k=the yield strength of the metal in shear).

$$\sigma_1 - \sigma_3 = \frac{2}{\sqrt{3}}\sigma_0 = Y = 2k \qquad [2.13]$$

$$\sigma_y + P = Y \Rightarrow P = Y - \sigma_x \qquad [2.14]$$

$\sigma_1 =$ algebrically largest principal stress

$\sigma_3 =$ algebricaly smallest principal stress

$\acute{\sigma_0} =$ yield strength of work material in plane stress

$\sigma_x = \sigma_1$ and $\sigma_3 = \sigma_y = -P$(−ve due to compression)

$\sigma_x - (-P) = Y \Rightarrow \sigma_x + P = Y$

differentiating and integrating the relation with respect to x, it gives

$$\frac{d}{dx}(\sigma_x + P = Y) = \frac{d\sigma_x}{dx} + \frac{dP}{dx} = 0 \Rightarrow \frac{d\sigma_x}{dx} = -\frac{dP}{dx} \Rightarrow \frac{dP}{dx} = -\frac{2K}{h}, \qquad \left(\frac{d\sigma_x}{dx} = \frac{2K}{h}\right)$$

$$\Rightarrow dP = -\frac{2K}{h} * dx \Rightarrow \int dP = \int -\frac{2K}{h} * dx \Rightarrow P = -\frac{2Kx}{h} + C \Rightarrow C = P + \frac{2Kx}{h}$$

using boundary condition , constant C can evaluated at x=a,$\sigma_x = 0, P = Y$

$$C = Y + \frac{2Ka}{h}, P = -\frac{2Kx}{h} + C \Rightarrow P = -\frac{2Kx}{h} + Y + \frac{2Ka}{h} = Y\left[1 + \frac{(a-x)}{h}\right], Y = 2K$$

At x=0,i.e, at the center of the work piece,the pressure(P) will be maximum.

$$P = P_{max} = Y\left[1 + \frac{a}{h}\right] \qquad [2.15]$$

At x=a,i.e,at the edge of the work piece,the pressure(P) will be minimum.

$$P = P_{min} = Y = 2K \qquad [2.16]$$

Average forging pressure acting over the interface between the die and the workpiece can be found by integrating p over half of the block to find the force and dividing that by the area of the half-block. This is valid from the edge (x=0) to the centerline (x=a). the area of the half block = half of the block width $*$ the block unit depth $= a * 1 = a$

$$\mathbf{P_{avg}} = \frac{F_y}{a} = \frac{1}{a}\int_{x=0}^{x=a} P dx = \frac{1}{a}\int_{x=0}^{x=a}\left[-\frac{2Kx}{h} + Y + \frac{2Ka}{h}\right] dx = Y\left[1 + \frac{a}{2h}\right]$$

$$\mathbf{F_{forging}} = (\mathbf{average\ forging\ pressure}) * \mathbf{area} = \left(\mathbf{P_{avg}}\right) * (\mathbf{2a} * \mathbf{L})$$

$$\mathbf{F_{forging}} = Y\left[1 + \frac{a}{2h}\right] * (\mathbf{2a} * \mathbf{L}) \qquad [2.17]$$

2.7.3.1 Expression for Forging Load in the Sliding Friction

When the friction is assummed to obey coulombs law,then $\tau = \mu P$,instead of $\tau = k$ where μ is coefficient of friction between the workpiece and the die and P is the forging pressure.Differentating the equation $\sigma_x + P = Y$ which is drived from the equilbrium equation in the y-direction with respect to x, the equation is expressed as follows.

$$\frac{d\sigma_x}{dx} + \frac{dP}{dx} = 0 \Rightarrow \frac{d\sigma_x}{dx} = -\frac{dP}{dx} = \frac{2\mu P}{h}, \qquad \left(\frac{d\sigma_x}{dx} = \frac{2\mu P}{h}\right)$$

$$\frac{dP}{P} = -\frac{2\mu}{h} * dx \Rightarrow \int \frac{dP}{P} = -\frac{2\mu}{h}\int dx \Rightarrow \ln P = -\frac{2\mu x}{h} + C$$

By using the boundary equation the constant,C can be evaluated at x= a, $\sigma_x = 0, P = \sigma_0'$

$$C = \ln Y + \frac{2\mu a}{h}, \ln P = -\frac{2\mu x}{h} + \ln Y + \frac{2\mu a}{h} \Rightarrow \ln P - \ln Y = \frac{2\mu}{h}(a - x) = \ln\frac{P}{Y} = \frac{2\mu}{h}(a - x)$$

$$\ln\frac{P}{Y} = \frac{2\mu}{h}(a - x) \Rightarrow \frac{P}{Y} = e^{\frac{2\mu}{h}(a-x)} \Rightarrow P = Y * e^{\frac{2\mu}{h}(a-x)}$$

$$\mathbf{P_{avg}} = \mathbf{P_{avg}} = \frac{F_y}{a} = \frac{Y}{a}\int_{x=0}^{x=a}\left[e^{\frac{2\mu}{h}(a-x)}\right] dx = -\frac{Yh}{2\mu a}\left[1 - e^{\frac{2\mu a}{h}}\right]$$

Assuming $\frac{2\mu}{h}$ to be small and Expanding as the taylor serie, $e^y = 1 + y + \frac{y^2}{2!}$+----,

$$\mathbf{P_{avg}} = \frac{Yh}{2\mu a}\left\{1 - \left[1 + \frac{2\mu a}{h} + \left(\frac{2\mu a}{h}\right)^2 * \frac{1}{2} + - - -\right]\right\} \approx Y\left[1 + \frac{\mu a}{h}\right]$$

$$\mathbf{F_{forging}} = (\mathbf{average\ forging\ pressure}) * \mathbf{area} = \left(\mathbf{P_{avg}}\right) * (\mathbf{2a} * \mathbf{L})$$

$$\mathbf{F_{forging}} = Y\left[1 + \frac{\mu a}{h}\right] * (\mathbf{2a} * \mathbf{L}) \qquad [2.18]$$

If the forging operation has both sticking and sliding force,the operation cannot approximated by one or the other,Then it need to include both in its pressure and average pressure calculations.

$$F_{forging} = F_{sliding} + F_{sticking} = (P_{ave} * A)_{sliding} + (P_{ave} * A)_{sticking}$$

$$F_{total} = Y\left[1 + \frac{\mu a}{h}\right] * (\mathbf{2a} * \mathbf{L}) + Y\left[1 + \frac{a}{2h}\right] * (\mathbf{2a} * \mathbf{L}) \ldots\ldots\ldots\ldots\ldots [2.19]$$

2.8 Finite element analysis for Forging process

Theoretical background of finite element analysis: For accurate finite element prediction of material flow during bulk metal forming, the formulation must take into account the large plastic deformation, incompressibility,workpiece-die contact, and temperature coupling. The basic equations to be satisfied are the equilibrium equation, the incompressibility condition and the stress-strain relationships[34].The equation of variation in the form:

$$\delta\phi(v) = \int_V \bar{\sigma}\, \delta\dot{\bar{\varepsilon}}\, dV + \int_V \dot{\varepsilon}\delta\dot{\varepsilon}_v dV + \int_S F_i \delta v_i dS = 0 \qquad [2.20]$$

In the mixed formulation, both velocity and pressure are solution variables. They are solved by the variation equation

$$\delta\phi(v,p) = \int_V \bar{\sigma}\, \delta\dot{\bar{\varepsilon}}\, dV + \int_V P\delta\dot{\varepsilon}_v dV + \int_V \dot{\varepsilon}_v \delta P - \int_S F_i \delta v_i dS = 0 \qquad [2.21]$$

where $\dot{\varepsilon}_v$ is the volumetric strain rate, $\bar{\sigma}$ is the effective stress, $\dot{\varepsilon}$ is effective strain, $\dot{\bar{\varepsilon}}$ is the effective strain rate, p is the pressure, V is the volume, and S is the surface of the deforming workpiece respectively.

Eq. [2.20] and [2.21] can be converted into a set of algebraic equations by utilizing the standard FEM discretization procedures. Due to the non-linearity involved in the material properties and frictional contact conditions, the solution is obtained iteratively.The temperature distribution of the workpiece and/or dies can be obtained readily by solving the energy balance equation rewritten, by using the weighted residual method, as

$$\int_V kT_{,j}\delta T_{,j} dV + \int_V \rho c\dot{T}\delta T dV \int_V \alpha\bar{\sigma}\delta\dot{\varepsilon}_v \delta T dV = \int_S q_n \delta T dS \qquad [2.22]$$

where k is the thermal conductivity, T is the temperature, ρ is the density, c is the specific heat, α is the fraction of deformation energy that converts into heat, and qn is the heat flux normal to the

boundary, including heat loss to the environment and friction heat between two contacting objects.

2.9 Simulation Software Selection for Forging Dies

The choice of finite element simulation software packages is very important for both the type of analysis that can be performed and the quality of the results. This is because different packages have different capabilities and it is critical to select the package with the appropriate feature set[35].

Table 2.3: finite element simulation software comparisons.

	DEFORM	AdvantEdge	Abacus
Ease of set up	Built in"wizards"for machining simulations. tool geometrie need tobe imported	Very fast setups. tool geometry libraries are provided	Manual design of workpies/tools.mesh refinment and boundary conditions have to be set manually.
Material models	Extensive material modellibraries. comprhensive material property editor	Extensive material model libraries. supportfor aerospace alloys.	None.no.material models present. but materials can be defined with a lot of details.
Adaptive meshing capabilities	Uses adaptive meshing.some control over the parameters.	Uses adaptive meshing, but controls cannot be modified	Partial support.not much fine control in adaptive meshing.
Overall control	Some level of control is permited.but basic FEM solvers cannot be manipulated.	Very minimal changes allowed.	Very high control.basic solverfunctioning can be modified.

2.10 Summary

In this study, a few selected research articles are reviewed and many researchers have tried to demonstrate the important part of finite element technology for the various deformation problems. Nowadays, different commercial forging simulation packages are available. Among the most widely used are DEFORM, MARC Auto Forge, MSC Super Forge, Forge 2 and 3, QForm, etc. They allow the simulation of cogging, rolling, forging and ring rolling in various way, extrusion, piercing and many of them are associated with heating and cooling processes.

The most important input parameters for modeling the forging process are the geometric (work-piece geometry and die geometry), the material properties, interface conditions (friction and heat transfer at the die-workpiece interface) and process parameters (the environment, the temperatures of work-piece and the die, the heat transfer coefficients between dies and the work-piece and the atmosphere, and the die velocity).

Due to the high temperatures and forming forces that arise in forging processes, dies are exposed to high thermal and mechanical loads. These loads have a major impact on the fatigue life of the dies and can therefore lead to formation of fatigue cracks on the surface. Due to the complex thermomechanical phenomena that occur in the interface layer between work-piece and forging die, it has not been possible to provide a reliable estimate of die life. To make a reliable estimate of die life, researchers have underlined the need for using advanced and sophisticated material models (numerical modeling software).

Based on the estimation of forging force, Analytical methods and numerical methods (simulation software) have been used in the literature to analyze the forging force and die performance. In analytical methods, metal forming problems are generally analyzed using three different methods such as the upper bound, slip line field, and slab method. The upper bound method was found to agree well with the finite element and experimental results.

2.11 Research gap

This study is conducted in Kotebe Metal Tools Factory for the purpose of fatigue life investigation and forging load optimization of the lower pickaxe die.The study is the first work performed on "***Fatigue Life Investigation for AISI-H13 used for the Application of Pickaxe Die using Numerical and Analytical Method"*** in the factory. No identical or similar work have been done before and untill the compeletion of this study. From the 64 publications used for hot forging process analysis in this study,non of them were adressed for pickaxe forging analysis except discussed the common methodology of forging process analysis for different process forged parts.

CHAPTER 3: MATERIAL AND METHODS

In this chapter, the material of the work-piece and the die have been selected.The geometrical model of the die and work-piece have been modelled using geometrical modelling software (SOLID WORK) and simulated using numerical simulation (DEFORM-3D) software.The forging load of the work-piece is calculated using analytical methods(slab and slip line methods) for validation (comparision purpose).With the help of the taguchi's experimental method,the results of the simulation experiment are optimized and the optimum forging process parameters are obtained. Finally, the fatigue life of the die is investigated using the ANSYS work bench.

3.1 Workpiece and Die Material

3.1.1 Material Used for Pickaxe Piercing die

The material of the die used in this study is made of chromium hot-work tool steel 8407 supreme (AISI-H13). It is the most reputable, hot work tool steel, especially for forging, giving a good toughness and high temperature strength, high hardenability and moderate wear resistance. "**Toughness"** is the ability of a material to absorb energy without fracture.H13 can resist thermal softening up to 550°C. "**Hardness"** is the resistance to wear, abrasion or indentation. The chemical composition of the materials specifically used for pickaxe die is listed in table 3.1.

Table 3.1: Chemical compositions of AISI H13 tool steel for Pickaxe die [36]

Components	**Mass (%)**
Carbon(C)	0.32-0.45
Chromium (Cr)	4.75-5.50
Manganese (Mn)	0.20-0.50
Molybdenum (Mo)	1.10-1.75
Vanadium(V)	0.80-1.20
Silicon (Si)	0.80-1.20
Copper (CU)	0.25
Phosphorus-sulfur(P-S)	0.03

Table 3.2: Mechanical and thermal properties of Pickaxe die [36]

selected Material	**AISI H13**
Young's modulus@ 20^{o}C	215GPa
Poisson's ratio	0.27-0.30
Tensile ultimate strength @ 20^{o}C	1200-1590 Mpa

Tensile yield strength@ 20^{o}C	1000-1380 MPa
Bulk modulus@ 20^{o}C	160Mpa
Elongation before fracture@ 20^{o}C	9%
Reduction of area@ 20^{o}C	50%
density@ 20^{o}C	7800kg/m^{3}
Melting point@ 20^{o}C	1427^{o}C
Thermal expansion	10.4*10^{-6} ^{o}C
Thermal conductivity	28.6 ^{o}C
hardness	
Knop	HK=570
Hardness Rockwell	HRC=45-48(46)
Brinell hardness 3000	BH=422-455
Vickers	Hv=549

3.1.2 Material Used for Billet

The material of the work piece used in this study is medium carbon steel (AISI 1045), and its chemical composition and physical and thermal properties are shown in Tables 3.3 and 3.4 respectively.

Table 3.3: Chemical compositions of AISI 1045 steel for billet (work piece) [36]

components	**Mass (%)**
Carbon(C)	0.35-0.49
Manganese (Mn)	0.5-0.8
phosphorus(p)	0.05
Silicon (Si)	0.15-0.35
Sulfur(S)	0.05

Table 3.4: Mechanical and thermal properties of AISI 1045 steel for work piece [36]

Material selected	**AISI 1045**
Young's modulus@ 20^{o}C	200 GPa
Poison's ratio	0.27
ultimate Tensile strength @ 20^{o}C	560 Mpa
yield Tensile strength@ 20^{o}C	275 Mpa
shear modulus@ 20^{o}C	75-80 Mpa
Elongation before fracture@ 20^{o}C	22%
Reduction of area@ 20^{o}C	50%
Table to be continued	

density@ 20^0C	7870kg/m^3
Melting point@ 20^{o}C	1520^{o}C
Coefficient of Thermal expansion	15 (µm/m ^{o}C)
Thermal conductivity	28.6 ^{o}C
Hardening temperature (Th)	760 ^{o}C
Tempering temperature (Tt)	400 ^{o}C

3.2 Geometry of the Die and Billet

3.2.1 Dimension of the Work-piece

The work-piece taken is rectangular as used in the factory and its dimensions are 30 mm thick, 60mm wide, and 157 mm long. The volume of the work-piece is 282,600 mm^3.The work-piece is inserted between the upper and lower dies to a cross section of approximately 157mm x 30 mm. Because the process involves open die forging, these geometrical dimensions can not be fully controlled.The dimensions of the work-piece may change for the consequent forging process.

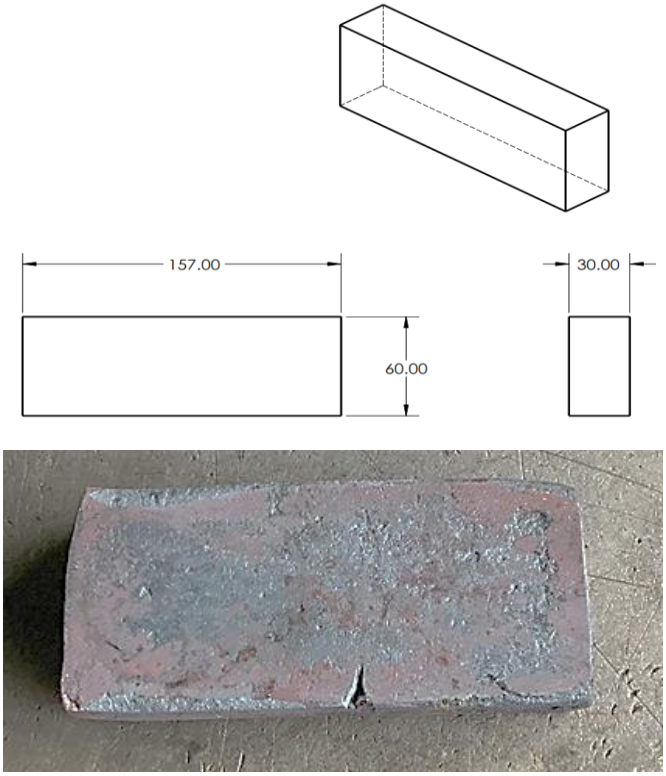

Figure 3.1: Dimension of work-piece

3.2.2 Dimension of the Upper (punch) and Lower Die

The dimensions of both the upper and lower dies were measured and recorded with an instrument during a site visit.Their dimensions are depicted in figure 3.2 and figure 3.3.As can be seen in the figure,the dies have a complex shape that would support the pickaxe after the forging process.

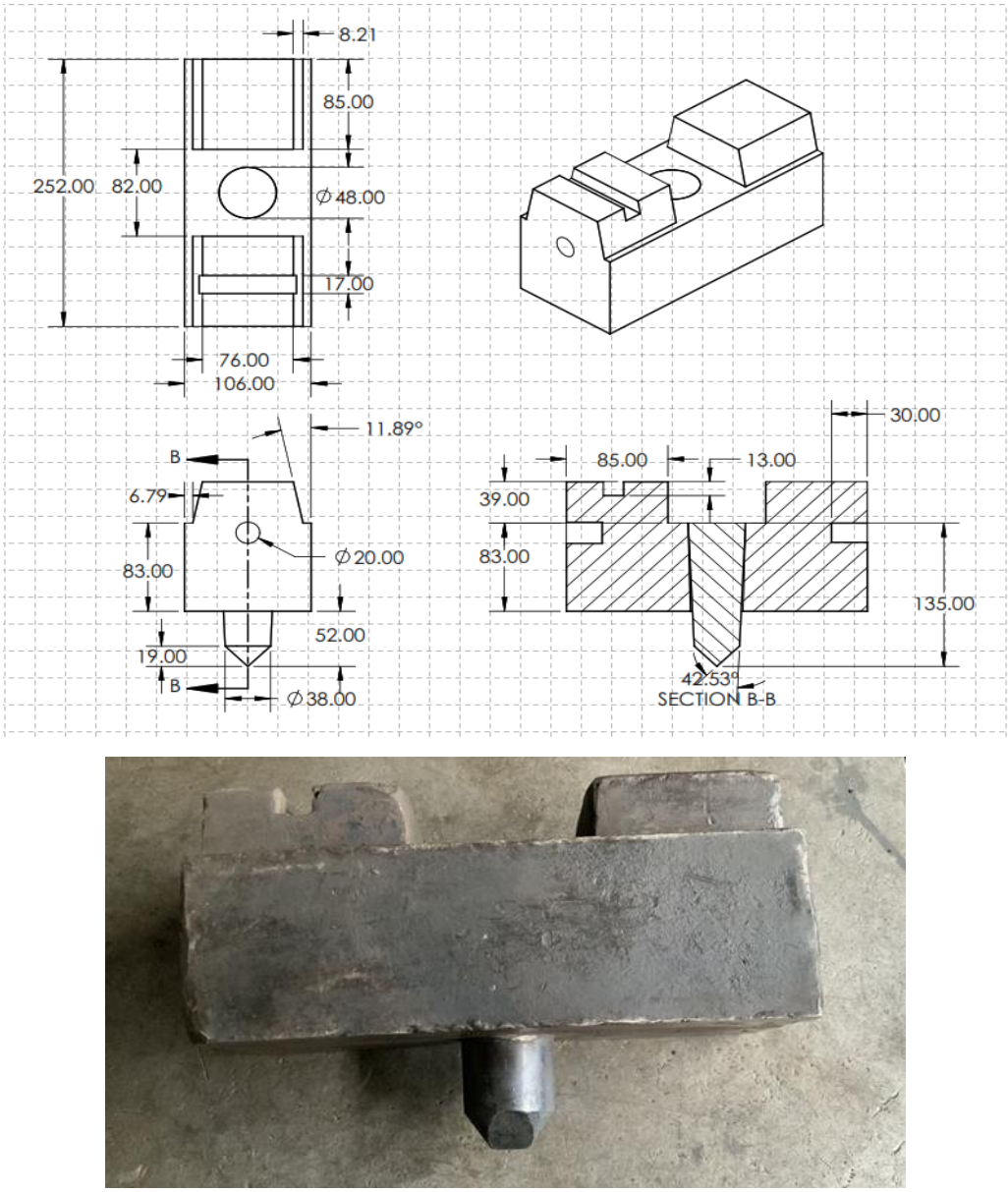

Figure 3.2: Dimension of the upper die punch

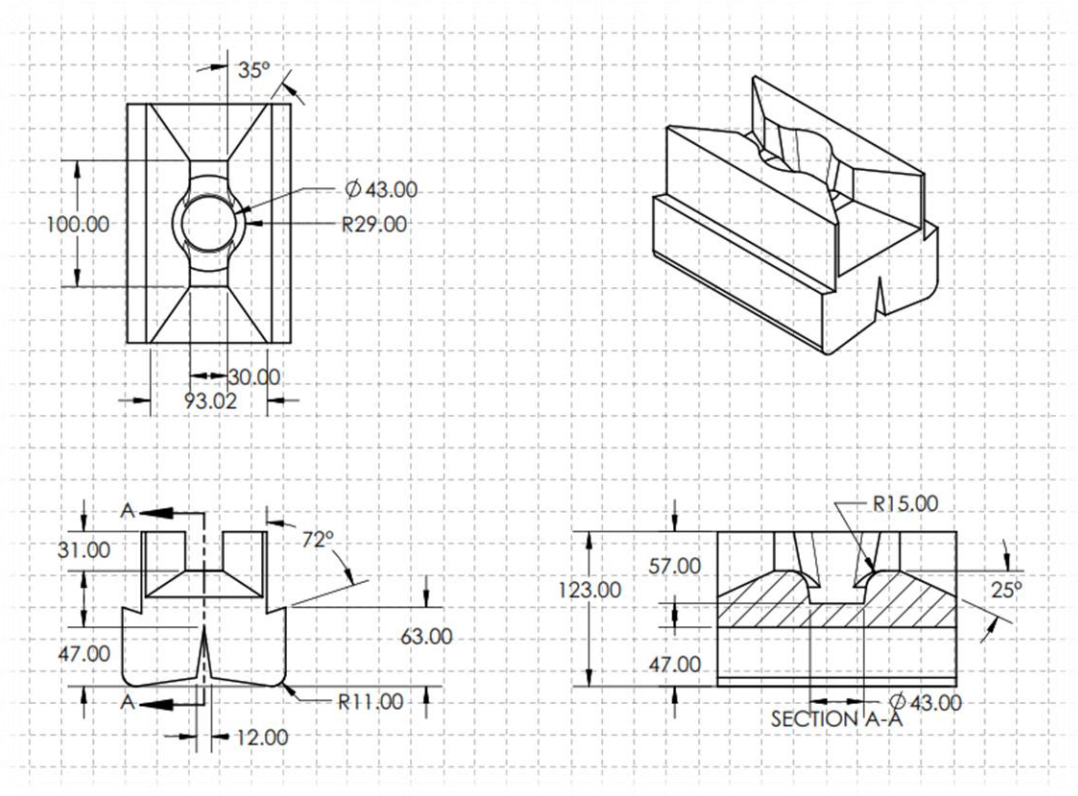

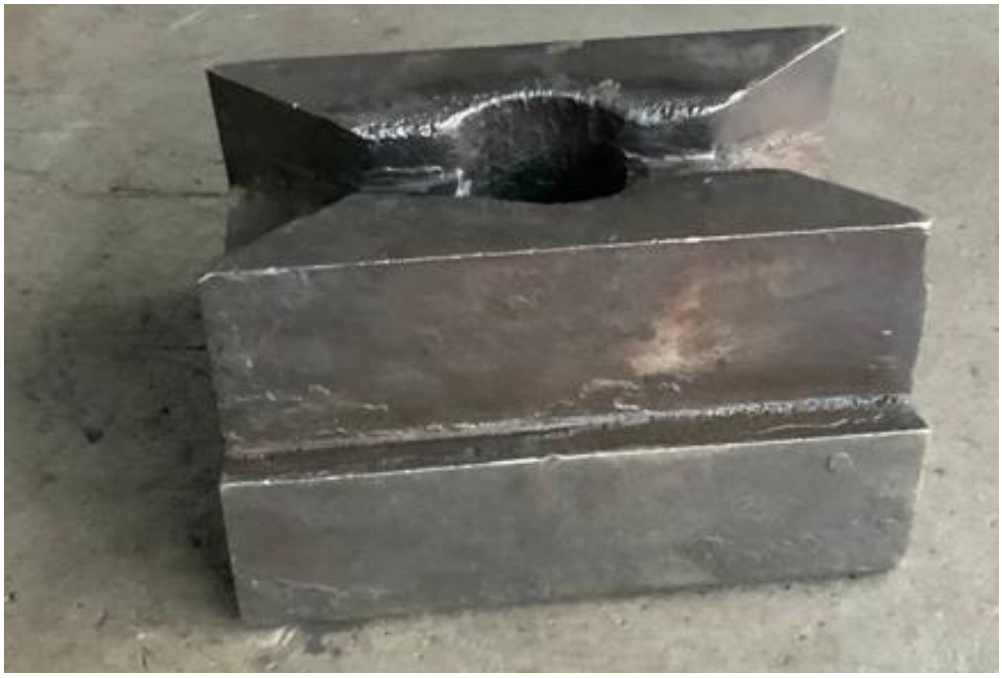

Figure 3.3: Dimension of lower die

3.3 Geometric Model for Workpiece and Dies

From a modeling point of view, all relevant tool components must be modeled from a geometric perspective. To carry out the FEM analysis of the forging process, it is essential to first develop the 3D-models of the workpiece and dies using apropriate modeling sofware that is compatible with metal forming simulation software such as DEFORM. Modeling software such as CATIA, proe.wildfire,solidwork are compatible with the DEFORM-3D sofwares[37].Figure 3.4 and 3.5 show the upper and lower forging die models for the pickaxe. The models were developed with solidwork 2020.

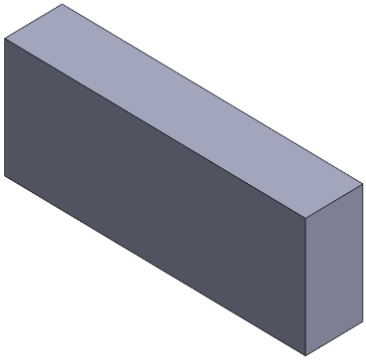

Figure 3.4: Geometrical Model of work-piece

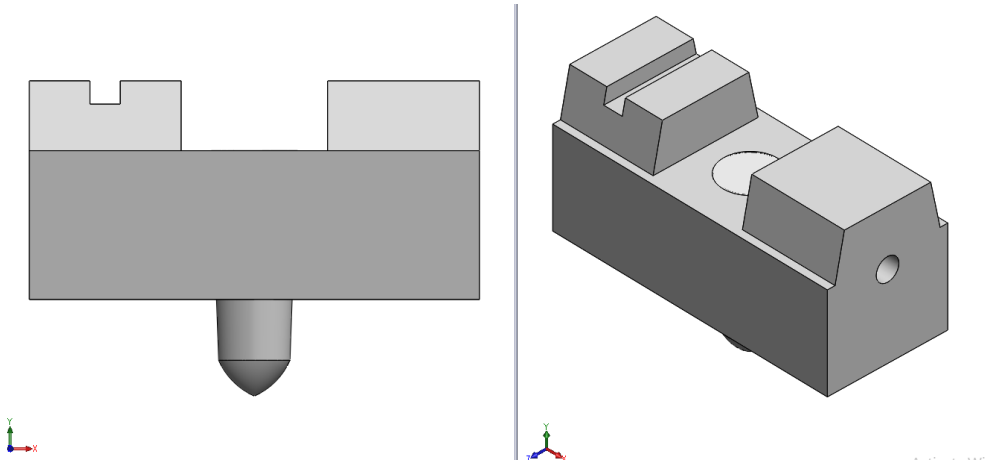

Figure 3.5: Geometrical Model of upper forging dies (punch)

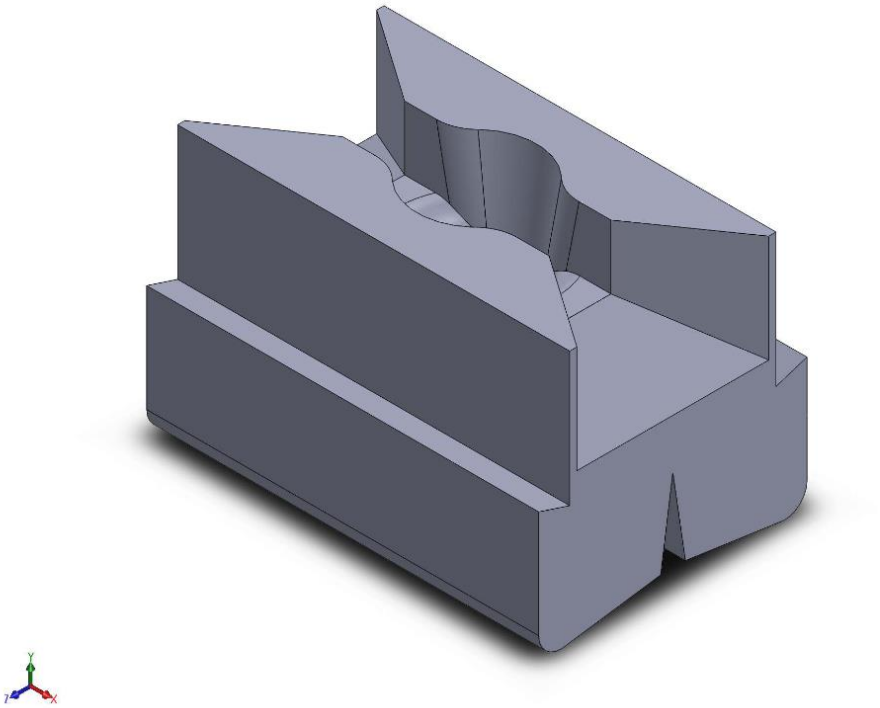

Figure 3.6: 3D-physical Model of lower forging die

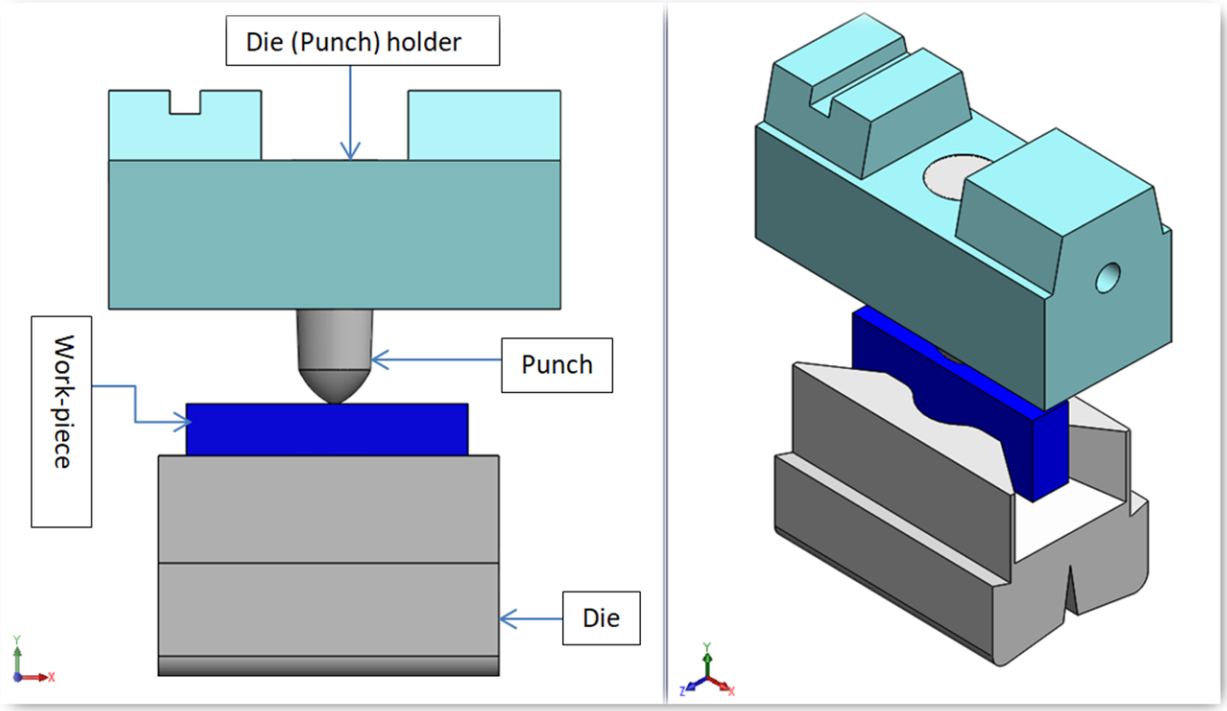

Figure 3.7: Geometrical model of the assembled die set

3.4 Conditions

3.4.1 Forging Method

In open die forging process, the work-piece, reheated to forging temperature, is placed on the lower die and pressed with the upper die to shape the final part. The upper die is attached to the ram and the lower die is attached to the press bed. Hot work(hot forging) is a hot forging process in which compressive forces in two dies are applied to a metal (work-piece) above the yield strength, resulting in plastic deformation of the work-piece. Hot forging is done at temperatures above the recrystallization temperatures, typically 0.6Tm or above, where Tm is the melting temperature of the work-piece. For this specific work, Triple crank press PK-300/100 with a nominal (rated) capacity of 300 tons and a stroke length of 200 mm was used for the hot forging process to manufacture pickaxe at Kotebe Metal Tools Factory. This general use mechanical press was designed for blanking, punching,drawing,bending and triming operation.The power source of the triple cranck press PK-300/100 is a large flywheel deriven by an electric motor.

The forging load behavior of crank press machines: There are two types of forging processes: impact forging (forging hammer) and press forging (crank press). In impact forging, the load is applied by impact, and deformation takes place over in a very short time. Impact loads are dynamic loads that are applied suddenly. The forging mallet can travel at speeds of up to 10 m/s, while the forging hammer acts through impact. In press forging, however, pressure is gradual buildup to cause the metal to yield. The time (duration) of application is relatively long. The longer forging process allows the material to cool down because the crank press's forging velocity is significantly lower, allowing the material to come into contact with the tool and the surrounding air. Crank presses therefore have no an impact effect and has static load effect at the end of the forging stage. when forging on a crank press, the strain field is more homogeneous than in hammer forging due to the quieter operation of the press and the lower forging velocities. The Spesfications for triple cranck press are listed in Table 3.5.

Table 3.5: Specification for triple crank press PK-300/100 [Figure 3.8.]

Rated pressure	300t
Pressure of cutter(trimer)	100t
Revolution of crank shaft	30 rpm
Stroke of cutter ram/constant/	136mm
Stroke of main ram/constant/	200mm
Max. distance between table and bottom surface of ram in its upper position	730mm
Distance between columns under the slide-ways	1000mm

3.4.2 Load and energy requirements in triple cranck press PK-300/100

The press with the parameters specified in table.3.5, is used to perform forging operation in which a rated pressure 300tons is applied over a distance of h=200mm(0.2m), the energy consumed during forging is calculated as follow:

$$\text{potential Energy} = \text{Work done} = \text{Force} * \text{distance} \Rightarrow W = F * S \quad [3.1]$$

$$\text{Force} = F = m * a \Rightarrow F = m * g \quad [3.2]$$

$$F = m * g = 300000 * 9.81 = 2943000\text{N} = 2943\ \text{kN}$$

$$\text{Work} = W = F * s \Rightarrow W = (m * g) * h = (2943) * 0.2 = 588.6\ \text{kJ}$$

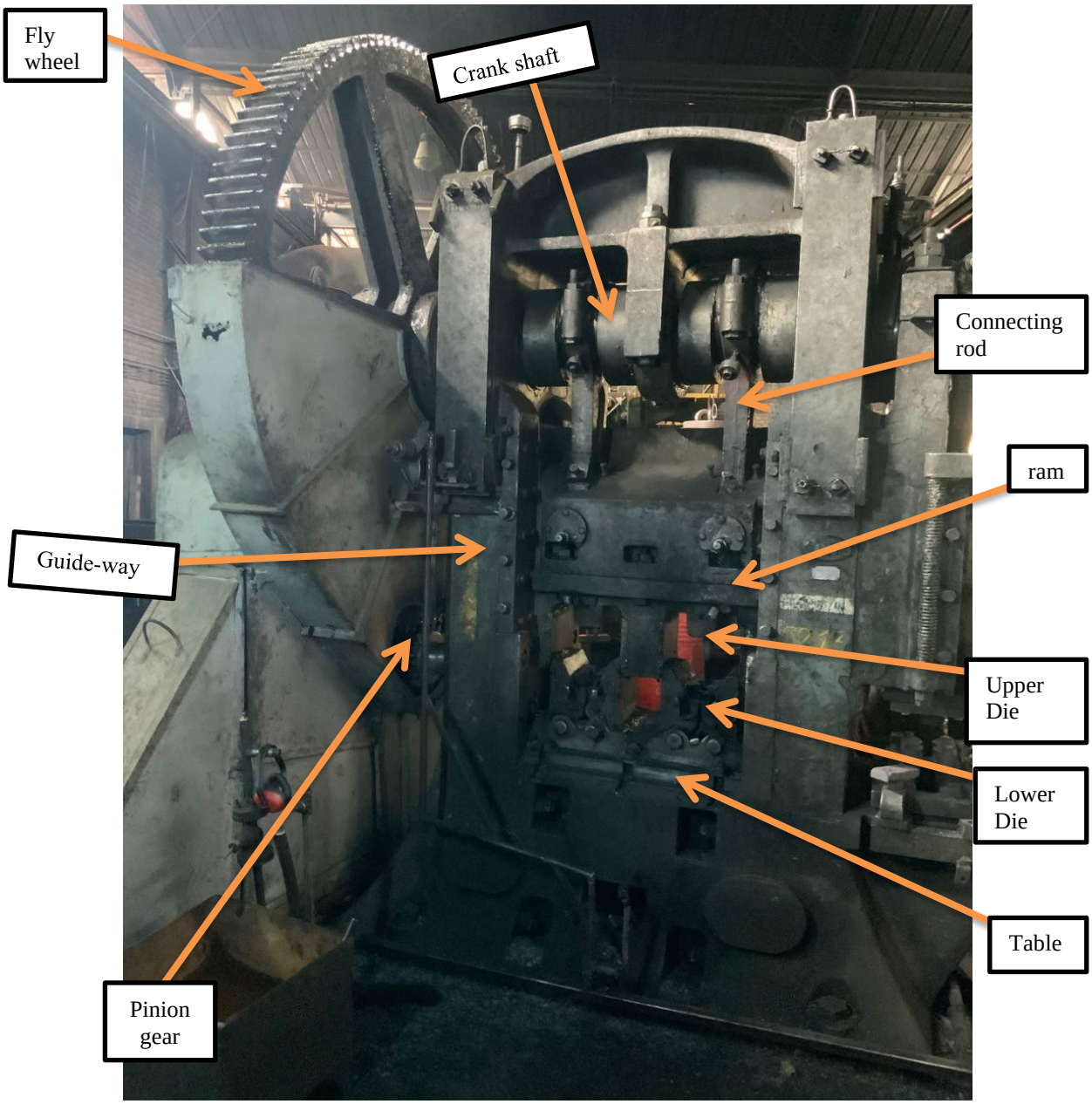

Figure 3.8: Triple crank press PK-300/100 machine.

3.5 Methods

The analytical method and numerical method were applied to analyze and identify the optimum(best) process parameter conditions for the deformation of AISI-1045 rectangular work-piece material througth the forging process. The analytical analysis was carried out using the slab and slip-line method to validate the result of the numerical method. The slab method was used to analyze the compressive load on the rectangular work-piece, which reduces the thicknees of the

work-piece.The slip-line method was used to analyze the piercing load in the rectangular work-piece to make a hole through the thickness.First, to investigate the fatigue life of pickaxe piercing die,it is mandatory to estimate the forging load and working temperature for the work-piece material. In this study, 3D-physical modeling software SOLID-WORK20.0 was used to model dies and work-piece geometry, and the finite element method-based numerical simulation software DEFORM-3D was used to simulate and estimate the forging load. The basic input data used for numerical simulation in DEFORM-3D software were die and workpiece materials, coefficient of friction between die and workpiece, thermal conditions (heat transfer coefficient), initial temperature of die and workpiece, ambient temperature, Stroke length, and ram velocity of the press machine.

ANSYS Workbench software, one of the ANSYS-Mechanical packages (used for structural and thermal analyses), was used to analyze the fatigue life of the pickaxe piercing die. Material properties include Young's modulus; Tensile yield stress, ultimate tensile stress, Poisson's ratio and density of AISI-H13 die steel were used as input material data for ANSYS Workbench simulation software.

The systematic organization of this study is represented in flow chart in figure 3.9

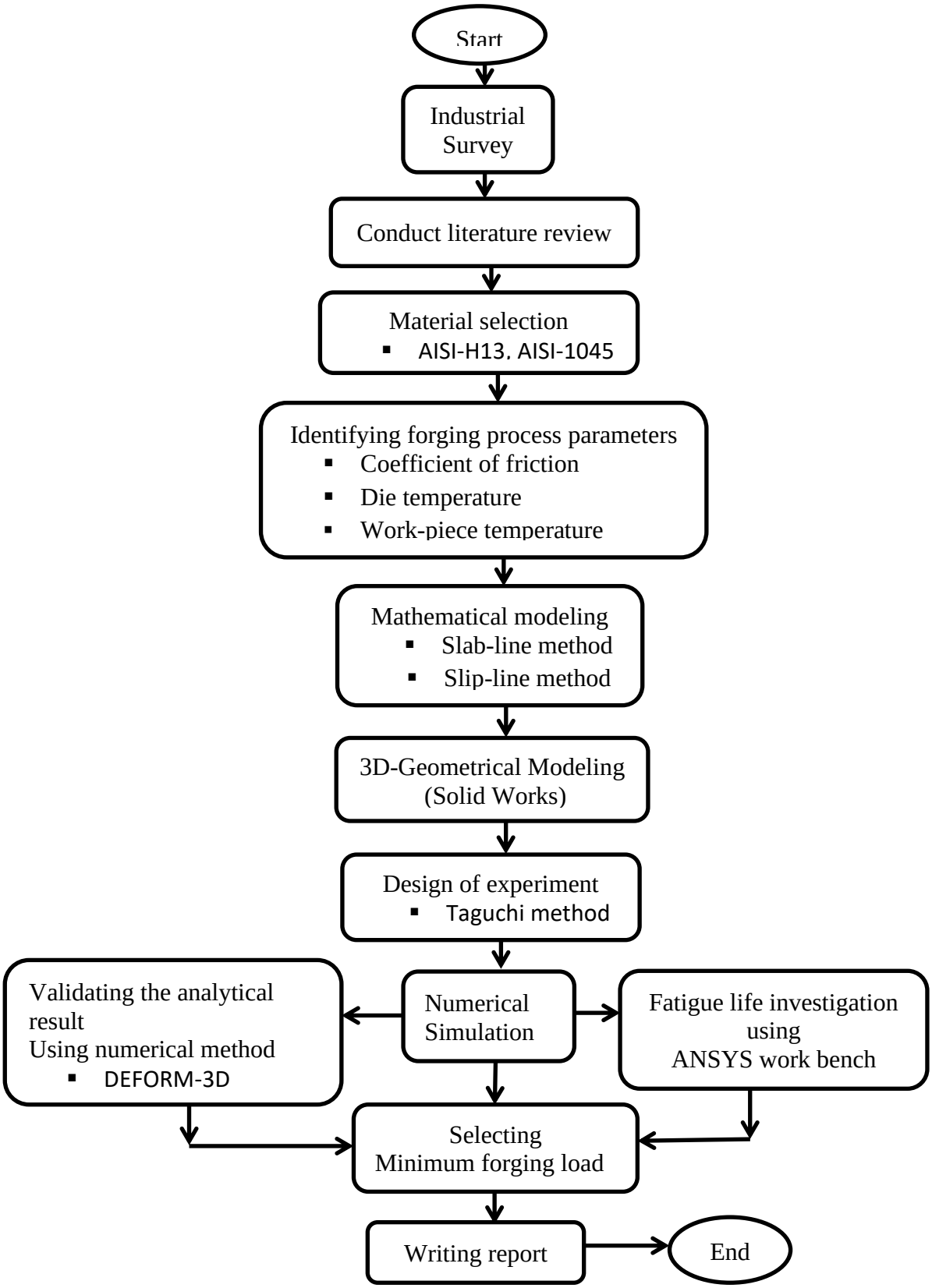

Figure 3.9: The systematic organization of the study

3.5.1 Design for Taguchi's Experiment

In this study, the Taguchi method has been applied to design the simulation experiment. The main objective of implementing this method in this study was to minimize the number of simulations run in order to reduce the computing time of the simulation software. And to analyze the best possible combination of simulation control factors (forging parameters. i.e., work-piece temperature, die temperature, and coefficient of friction) to obtain an accurate interrelationship among parameters and their influence on the pickaxe forging process. Based on the Taguchi method, the orthogonal experimental design of pickaxe forging is designed by taking pickaxe forging process parameters (work-piece temperature, die temperature, and coefficient of friction) as experimental factors and optimizing the pickaxe forging load as experimental objective. During the forging process, the following Parameters (main control factors) are considered for this study: die temperature, work-piece temperature, and coefficient of friction.

2.5.2 Optimization process

The goal of the optimization process is to find the best solution for the given problem (forging process). Optimizing the forging process is very essential to making the process efficient. In general, the parameter optimization process of the Taguchi method is based on 8-steps of planning, conducting and evaluating the results of matrix experiments to determine the best control parameters levels[15, 38]. These eight steps are described as follows.

1. Identify the performance characteristics (responses) to be optimized and the process parameters to be controlled (test).
2. Determine the number of levels for each of the tested parameters.
3. Select an appropriate orthogonal array, and assign each tested parameters into the array.
4. Conduct a random experiment based on the arrangement of the orthogonal array.
5. Calculate the S/N ratio for each combination of the tested parameters.
6. Analysis the experimental result using the S/N ratio and ANOVA test.
7. Find the optimal level for each of the process parameters.
8. Conduct the validation experiment to verify the optimal process parameters.

The steps of Taguchi method are shown in flow chart form in figure 3.10.

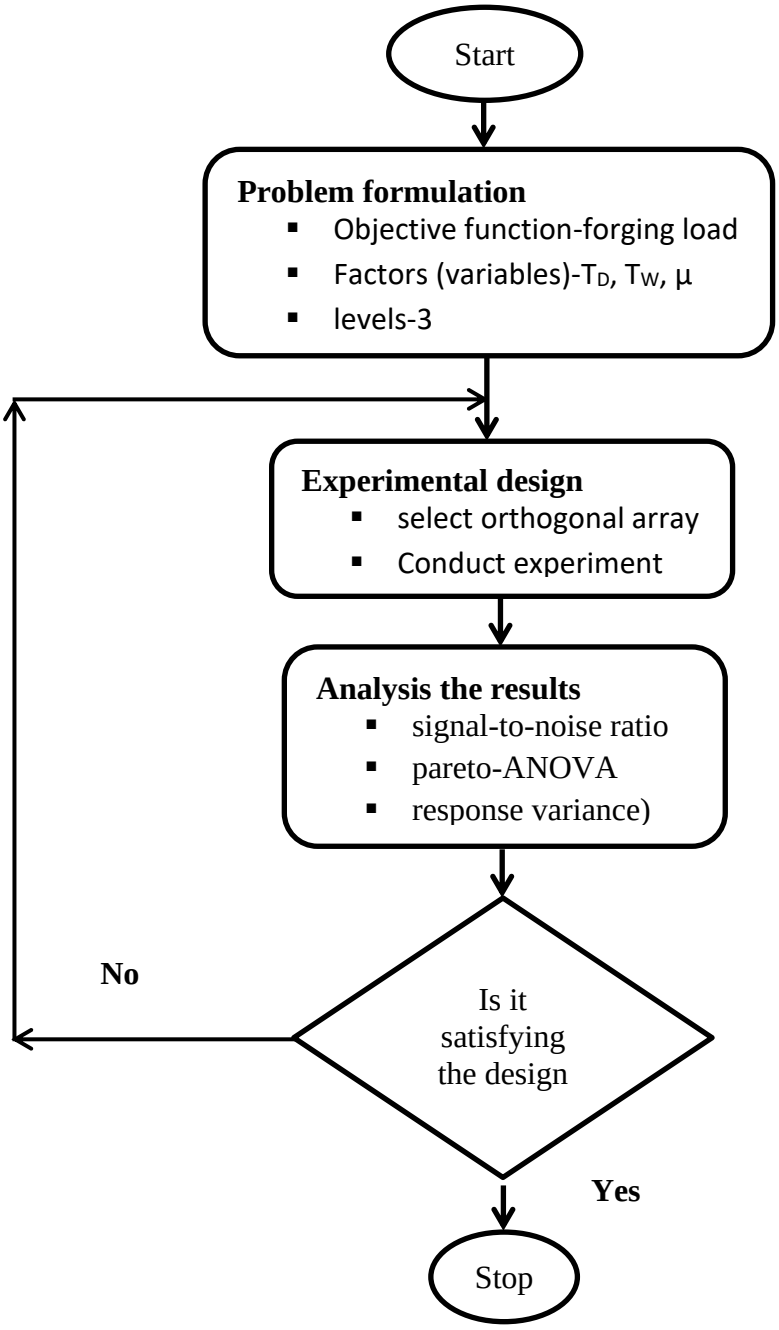

Figure 3.10: Flow diagram of Taguchi method

3.5.3 Design for experimental factors and levels

In the forging process, the contact between the die and the work-piece causes a drop in the work-piece temperature, leads to an increase in the metal flow stress of the work-piece, and difficult to the forging process. At the same time, the temperature difference at contact surface between the

die and the work-piece will cause thermal stress on the pickaxe piercing die, affecting the life of the die and the quality of forging. Therefore, there is a need to analyze the preheating temperature of the pickaxe piercing die. The friction between the die and work-piece reduces the metal flow, and the coefficient of friction directly affects the homogeneity of the deformation.

Therefore, in this study, work-piece temperature, die temperature, and friction coefficients were selected as three experimental factors (experimental design parameters). Each of the experimental factors has three level values (work-piece temperature: 900, 1000, 1050, die temperature: 150,200,250, and coefficient of friction: 0.3, 0.5, 0.7). Thus, a three-level orthogonal array (OA) was used in table3.6 resulting in 27 sets of simulations.

Table 3.6: Simulation control factors and their different levels

Levels	Factors/parameters	Levels value		
A	Work-piece temperature(^{0}C)	900	1000	1050
B	Lower- die temperature(^{0}C)	150	200	250
C	Friction coefficient(μ)	0.3	0.5	0.7

Based on the Taguchi method, the best possible combination of simulation control factors was analyzed using MINITAB software for the desired response (forging load) and examined using three-level full factorial design of experiments.

Table 3.7: Taguchi's experimental design with full factorial (L27) orthogonal design array.

simulation run	Simulation control factors					
	Uncoded values			Coded values		
	A	B	C	A	B	C
R1	1	1	1	900	150	0.3
R2	1	1	2	900	150	0.5
R3	1	1	3	900	150	0.7
R4	1	2	1	900	200	0.3
R5	1	2	2	900	200	0.5

Table to be continued

R6	1	2	3	900	200	0.7
R7	1	3	1	900	250	0.3
R8	1	3	2	900	250	0.5
R9	1	3	3	900	250	0.7
R10	2	1	1	1000	150	0.3
R11	2	1	2	1000	150	0.5
R12	2	1	3	1000	150	0.7
R13	2	2	1	1000	200	0.3
R14	2	2	2	1000	200	0.5
R15	2	2	3	1000	200	0.7
R16	2	3	1	1000	250	0.3
R17	2	3	2	1000	250	0.5
R18	2	3	3	1000	250	0.7
R19	3	1	1	1050	150	0.3
R20	3	1	2	1050	150	0.5
R21	3	1	3	1050	150	0.7
R22	3	2	1	1050	200	0.3
R23	3	2	2	1050	200	0.5
R24	3	2	3	1050	200	0.7
R25	3	3	1	1050	250	0.3
R26	3	3	2	1050	250	0.5
R27	3	3	3	1050	250	0.7

3.5.4. Signal to Noise (S/N) ratio calculation

Depending on the end objective (desired outcome), there are three methods available for calculating the S/N ratio: the lower-the-better, the higher-the-better and the nominal-the-better.

1. **Smaller-the-better:** when the interest is to find the best parameters to get the minimum amount of the desired product.

$$S/N = -10\log_{10}\frac{\sum Y_i^2}{n}$$

2. **Larger-the-better:** when interest is to find the best parameters to get the largest amount of the desired product.

$$S/N = -10\log_{10}\frac{1}{n}\sum\frac{1}{Y_i^2}$$

3. **Nominal-the-better:** when interest is to find the best parameters to get the exact amount of the desired product.

$$S/N = -10\log_{10}\left(\frac{\overline{Y}}{S^2}\right)$$

Where Y_i=the mean response calculated as $y = 1/n\,\Sigma Y_i$ and n=the number of experiments carried out under similar conditions. Since this was an interest in getting the low forging load, smaller-the-better technique has been selected in this study.

3.6 Modeling and simulation of the material flow in forging process

Due to non-steady state and non-uniform (uneven) material flow, significant interface friction and heat transfer between the deformed work-piece and the die, it is very difficult to analyze the forging load using mathimatical model. Due to these limitations (constraints) , a numerical method is used to estimate the forging load of the pickaxe work-piece.The most important input parameters for modelling the forging process are the geometric, the materials and process parameters.

3.6.1. Geometric parameters

Depending on the complexity of the imported 3D-physical models, it is possible to simulate the forging process as a three-dimensional, axisymmetric (plane-strain), and two-dimensional problem. A three-dimensional simulation problem was taken into consideration in this study. The developed geometric model of this study is depicted in Figure 3.4-3.7.

3.6.3 Material description

In order to accurately predict material flow and forging loads,it was mandatory to use material input data. The material of the rectangular workpiece is AISI 1045 medium carbon steel,while AISI H13 die steel is used as the material for the top die (primary die) and bottom die (secondary die).The imported 3D-physical model of the dies and the work-piece was considered as rigid and plastic models respectively.The mechanical properties and their detailed material data are shown in table 2.1and 2.2.

3.6.4 Interaction and Boundary condition

Contact boundary conditions define the y-interobject boundary contact conditions for a given loading condition object.Contact boundary conditions were applied to nodes of a slave object (work- piece), and specified the contact between these nodes and the surface of a master object (top die). In the mechanics boundary condition(friction), the coefficient of friction between the workpiece and the die was 0.3 (lubricated condition) ,0.5 and 0.7(dry condition). In thermal boundary condition(heat transfer), the conduction and convection coefficients were 5N/sec/mm/^{o}C and 0.02N/sec/mm/^{o}C respectively.

For the temperature boundary condition, the initial temperature of the work-piece is 900-1050^{o}C. The initial temperature of the die is 150-250^{o}C. The ambient temperature of the workpiece and the dies was 20^{o}C. In movement boundary condition, the bottom die and work-piece have no movement(stationary).They come into contact while the uper die just approches the work-piece and the movement of the upper die is performed by means of the mechanical crank press. The linear movement of the punch takes place in the y-axis with a forging speed and a stroke length of 54.5mm/s and 74mm respectively.

3.7 Numerical simulation of forging process

DEFORM-3D simulation software has been used in order to understand metal flow in the deformation process. In the DEFORM 3D software package, the Simulations are performed in the “Hot Forging” option. The meshing of the billet is done by the software into 20,000 elements. The maximum size of one element was 2.25mm. The total number of elements for the whole assembly was just over 84,000 pieces. Figure 3.11 shows the simulation of the forging process on a rectangular billet.

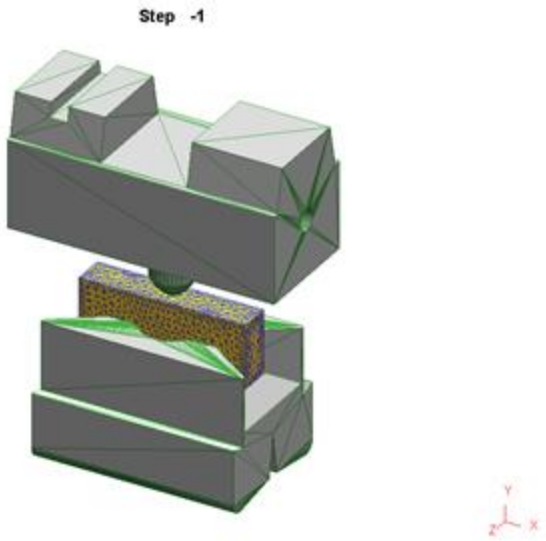

Figure 3.11: DEFORM-3D meshed simulation model

3.7.1 Simulation of the forging of end pickaxe

Different simulations are carried out at different temperatures (900°C, 1000°C, and 1050°C.) The objective of these simulations is to determine the optimum temperature and forging load for the forging process of this component. The number of forging operation step was set at 250 with the write interval of each 20 step and the step increment was 0.015 sec/. The simulation calculation stops when the distance between the upper and lower dies riches 10 mm.

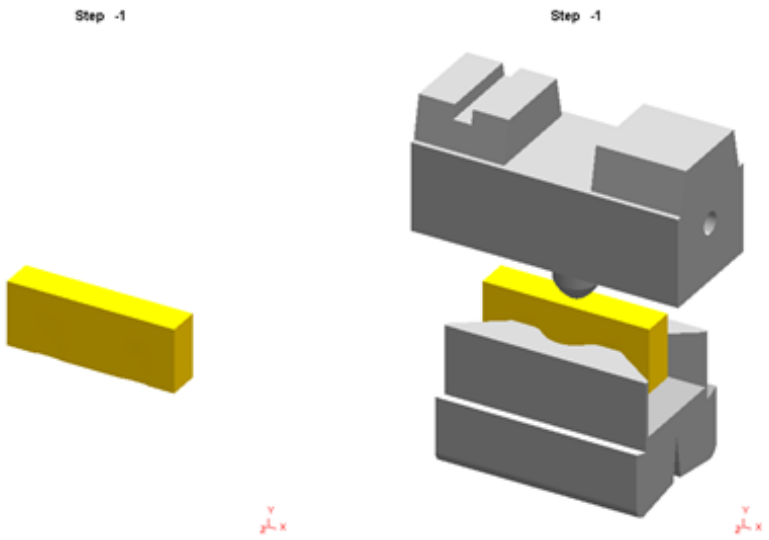

Figure 3.12: work-piece, lower die, and upper die setup before forging process.

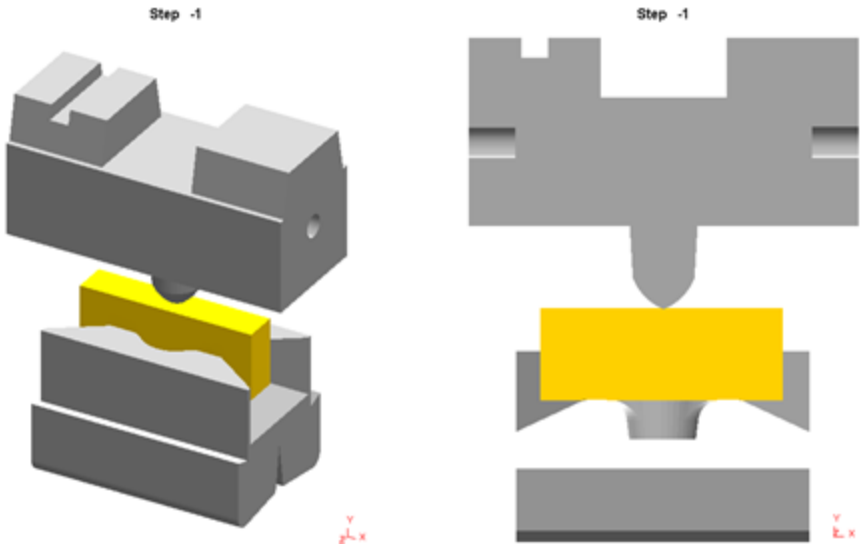

Figure 3.13: sectional view of work piece lower die, and upper die setup before forging process

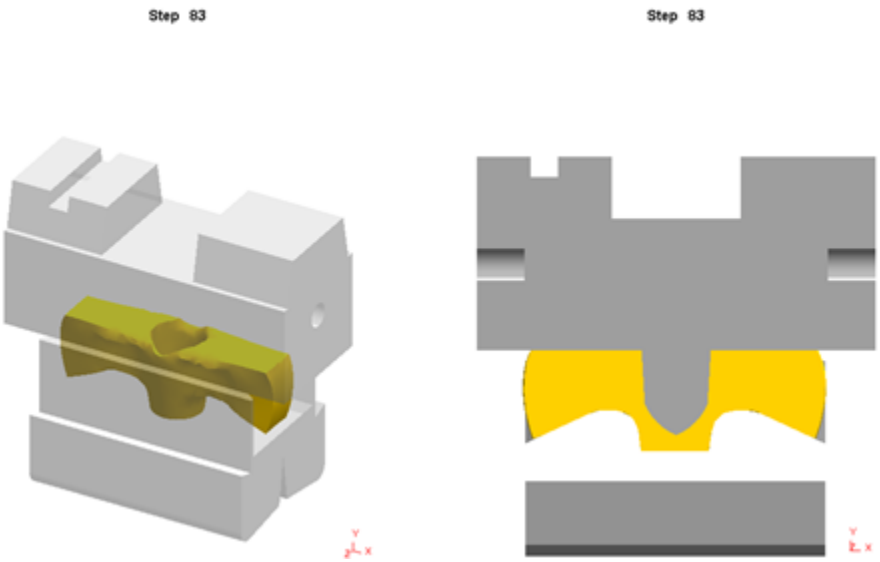

Figure 3.14: Sectional view of work piece lower die, and upper die setup after forging process

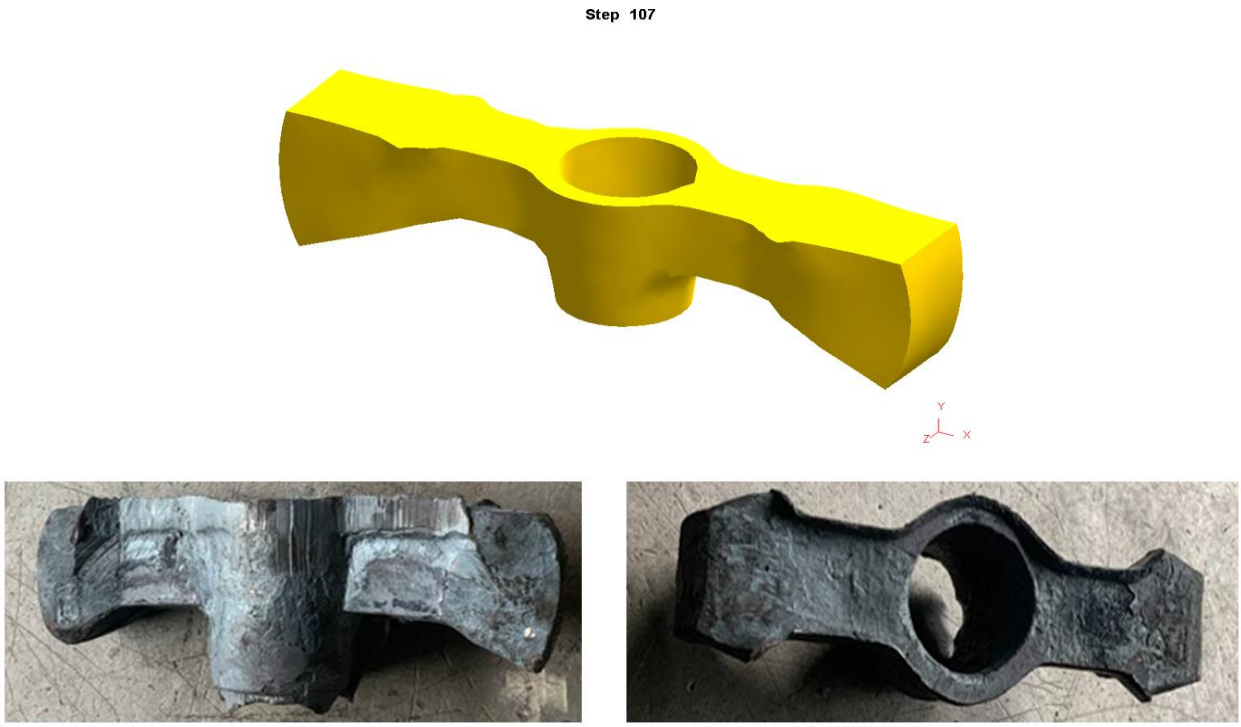

Figure 3.15: forged work piece of pickaxe after trimming operation.

3.8 Numerical simulation for fatigue life investigation

3.8.1 Introduction to fatigue

In this study used Fatigue Analysis: Stress Life have methodsbeen. The fatigue life investigations of the pickaxe die without defects (crack) is performed by using strength of material theory, which depends on the relationship between the applied stress (due to the applied forging load) and the material strength (ultimate tensile stress). To investigate the fatigue life the lower die of pickaxe, numerical simulations were carried out in the ANSYS workbench based on finite element analysis. In study, the fundamental steady state structural solver is used.

3.8.2 Finite element analysis parameters and methods

In order to perform a finite element analysis, it is not enough to simply run the simulation in an available finite element software, bu it is more important to understand the method behind the analysis. There are certain parameters that control the accuracy of the finite element analysis (FEA), such as model simplification,mesh size, element type and accuracy percentage. By

understanding the impact of the above parameters, it is possible to run the simulation efficiently[39].

3.8.2a 3D-physical Modeling of pickaxe piercing die.

Because of the complexity of the shape of the pickaxe piercing die, the 3D model of the pickaxe piercing die was modeled by Solidwork and then imported into ANSYS R19 Workbench for further analysis.

3.8.2b Material Properties

The material selected for the analysis of the pickaxe piercing die is AISI-H13 steel,which is used for the hot working die.The required properties for fatigue life analysis are given in Table.3.8

Table 3.8: mechanical properties of AISI-H13 die steel

Tensile yield strength,σ_y(Mpa)	ultimate Tensile strength, σ_{ut}(Mpa)	Young's modulus,E(GPa)	Poisson's ratio(ν)	Density, ρ(kg/m^3)
1380	1590	215	0.30	7800

3.8.2c Mesh generation

Element size: In order to achieve accurate results in simulation, it is essential that the finite element model is well prepared and has the appropriate element size and nodes. The size of the mesh element is inversely proportional to the simulation time and accuracy of the results. In order to obtain reliable results in a shorter simulation time, an optimal mesh element size should be achieved. A mesh that is too caorse (rough) will lead to incorect results. On the otherhand, a mesh that is too fine could lead to longer CPU computig time without a corresponding increase in accuracy.An experimental simulation was performed by employing an element size of 2mm for the input parameter and obtaining the corresponding output parameters(total deformation), which are further used to establish the functional relationship between the input and output.

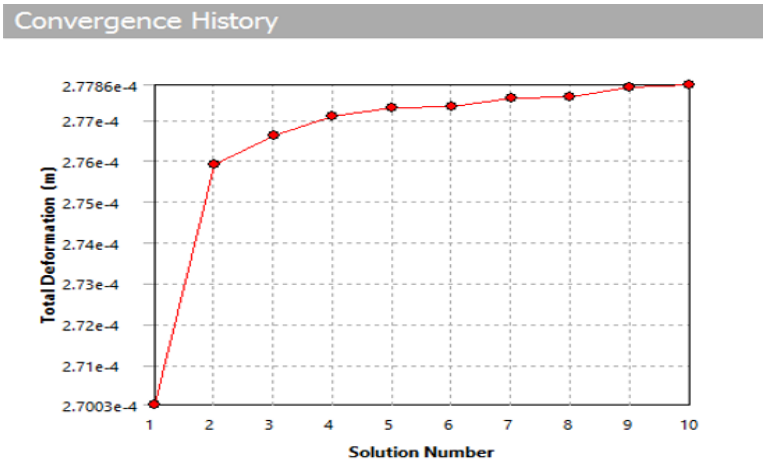

	Total Deformation (m)	Change (%)	Nodes	Elements
1	2.7003e-004		112303	56001
2	2.7591e-004	2.1525	290443	183215
3	2.7662e-004	0.25704	462318	308114
4	2.7709e-004	0.16933	683057	466159
5	2.7731e-004	7.8434e-002	1262333	881135
6	2.7732e-004	6.6428e-003	1320943	922745
7	2.7753e-004	7.3424e-002	2711585	1924880
8	2.7755e-004	7.3483e-003	3037744	2158655
9	2.7779e-004	8.8196e-002	6348090	4548352
10	2.7786e-004	2.3811e-002	11178646	8039195

Figure 3.16: mesh convergence analysis

Element type: Elements have ideal shapes when there is little or no error in the numerical computation of the individual stiffness matrices.However, it is almost impossible to model complex systems with a mesh of ideally shaped elements. Therefore, it is advisable to match (adjust) the mesh density to accomodate stress gradients and deformation patterns which imply that elements vary in size,have unequal side lengths and are warped or tapered.Hexahedrons are better suited for structural analysis than tetrahedral mesh elements to increase the accuracy of the result.But it is tedious and time-consuming to build a finite element model of the pickaxe piercing die with hexahedrons. Due to the complexity of the shape of the pickaxe piercing die,tetrahedral mesh elements were used for this study.

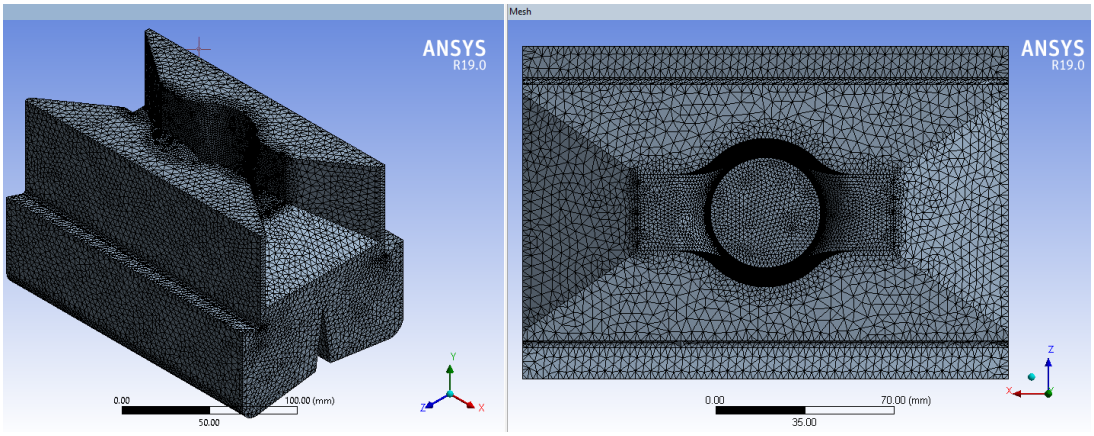

Figure 3.17: meshed pickaxe piercing die mode

3.8.3 Boundary Conditions

After meshing the lower pickaxe piercing die, the boundary Conditions in the model must be applied.The static load analysis was performed considering two boundary conditions. The bottom and side surfaces of pickaxe piercing die are fixed (constrained) to prevent the model from moving when the forging load is applied to the top of the lower pickaxe piercing die. The bottom of the lower die is fixed to the press bed. After fixing the model, the calculated forging load of 2.92MN is applied to the top surface of the pickaxe piercing die as inputs for the analysis.

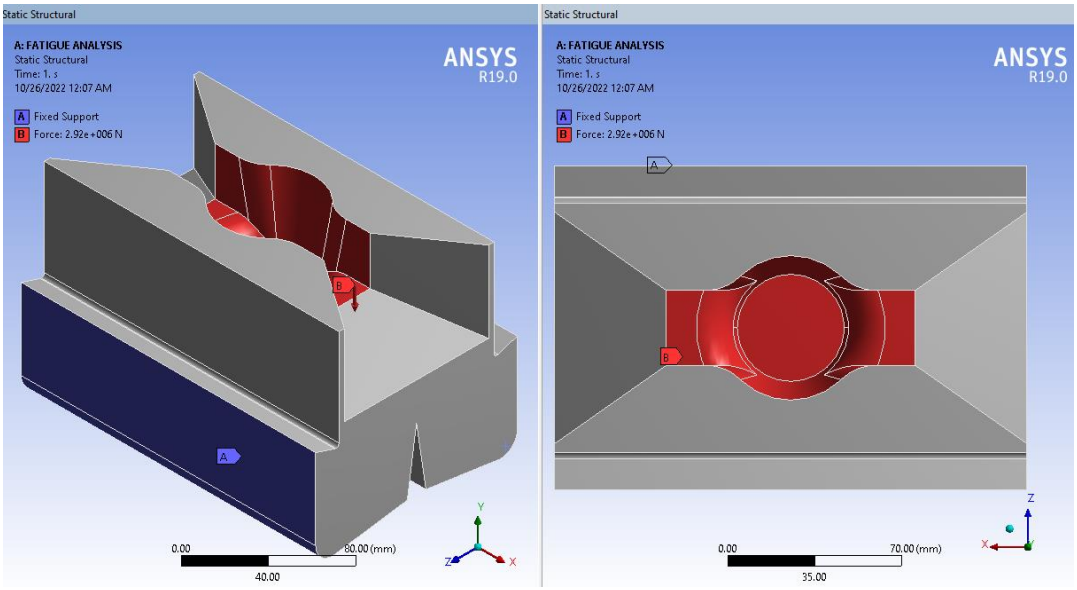

Figure 3.18: boundary and loading condition of pickaxe piercing die

In this study, the common decisions used to analysis fatigue life of the die are

1. fatigue analysis type-***Stress Life***
2. cyclic loading type-***Constant amplitude, proportional loading***

   The die stresses at each cycle vary from zero to a maximum and back to zero so the load of opposite sign does not occur. Also the peak loads can be considered as constant.
3. Mean Stress Effects- ***multiple S-N curves (experimental data***)
4. Multiaxial Stress Correction-***Component Y***
5. Fatigue Modification Factor-***Log-log***

3.8.4 Determination of S-N curve for AISI-H13 hot forging die steel

The Wohler approach, also known as the stress-life approach, displays data using log-log plots of stress against cycles to failure. The material's Wohler curve serves as the foundational information for the analysis of fatigue calculations. The S-N method does not work well in low cycle applications where the applied strains have a significant plastic component. This method neglects the actual stress-strain behavior and treats all strains elastically and does not separate the crack initiation phase from the propagation phase. Therefore, the simplified assumptions of the S-N approach are valid only when the plastic strains are small (in some cases they are actually too small to measure). This is particularly important in forging dies where mechanical failure can be the result of plastic deformation. In order to perform life simulation for the pickaxe piercing die, data from fatigue tests in the form of a Wohler curve of the die material must be loaded into the software. On the ANSYS workbench by default displays the S-N curve of structural steel, but the material used in this study is AISI-H13 Steel. The S-N curve of this material is shown in Figure 3.21.

Determination of S-N curve: the S-N curve (also known as Wohler curve) represent statistical models that characterizes the material performance. For the purpose of obtaining the most probable *S-N* curve, the following equation is applied in this study.

$$\sigma - \sigma_e = AN^m \Rightarrow S_{(N)} = AN^m \quad (m < 0) \qquad [3.1]$$

where N is a number of cycles to fracture under a repeated stress, S is fatigue strength (alternating stress), σ_e is the endurance limit, and A and m are arbitrary constants[40]. Taking the common logarithm of both sides of Eq. [3.1], then it gives

$$\log_{10}(S) = \log_{10}A + m\log_{10}(N) \qquad [3.2]$$

By transforming variables by the following substitution, the following relation is obtained:

$$\left.\begin{matrix}\log_{10}A = b \\ \log_{10}(S) = y \\ \log_{10}N = x\end{matrix}\right\} \Rightarrow y = mx + b \Rightarrow \log_{10}(S) = m\log_{10}(N) + b$$

Here the correlation between x and y becomes linear. Thus, the S-N curve values of this material can be solved using the generalized S-N formula.

$$\log_{10}(S) = m\log_{10}(N) + b \qquad [3.3]$$

The two constants m and b are unkown,and can be determined from the following relationship. The approach assumes that two points on the plot are required for the determination of fatigue characteristics: the fatigue limit (S_e) for the basic 10^6 cycles (N_{knee}) for steel and the fatigue for 10^3 cycles (N_{up}). The fatigue life given as the number of cycles for any alternating stress S_a can be calculated from the above Wohler Equation by applying two boundary conditions[41]:

$S(N) = S_m \;\; at\; N = 10^3$ cycles , and $S(N) = S_e \;\; at\; N = 10^6$ cycles. By substituting those values in eq.[3.3],the following two equations can be obtained.

$$\log_{10}(S_e) = m\log_{10}(10^6) + b \qquad [3.4]$$

$$\log_{10}(S_m) = m\log_{10}(10^3) + b \qquad [3.5]$$

solving for m and b from equations [3.4] and [3.5],then the values of m and b expressed as:

$$m = \frac{1}{3}\log_{10}\left(\frac{S_e}{S_m}\right), \quad and \quad b = \log_{10}\left(\frac{{S_m}^2}{S_e}\right) \qquad [3.6]$$

By substituting the values of m and b in eq [3.2],the general S-N equation expressed as:

$$\log_{10}(S) = \frac{1}{3}\log_{10}\left(\frac{S_e}{S_m}\right) * \log_{10}(N) + \log_{10}\left(\frac{{S_m}^2}{S_e}\right) \quad [3.7]$$

The corresponding fatigue strength (alternating stress) can be found by substituting any value of number of cycles(N) in equation [3.7].first, S_m and S_e are calculated depending the mechanical properties and loading condions of AISI-H13 die material.

Mean and endurance stress calculation: The endurance limit is the amplitude of the cyclic stress that can be applied to the material without causing fatigue failure. To establish the relationship of die fatigue life with die stress and the material properties of the die, Goodman equation is not used, because forging dies are loaded and then completely unloaded, they ideally have ratios of R=0 and A=1, this means that using Gerber or Goodman's equations to deduce the cycles till failure is useless. Therefore, the graphical approach was used and endurance limit was estimated as $\acute{S_e}$=0.5*S_u, for S_u<1400Mpa and $\acute{S_e}$=700Mpa, for S_u>1400Mpa. From the S-N diagram, the die fatigue life can be determined based on the given amplitude and mean stresses.

The proposed S-N curve relates the logarithm of the stress range to the logarithm of the number of cycles to failure in the medium and high cycle fatigue range under constant amplitude loading. Figure 3.20 depicts the S-N curve corresponding to steel. If the cycle stress of approximately 1431 MPa is applied to the die steel, the failure will occur after 10^3 cycles. Furthermore, at 795 MPa the S-N curve reaches the endurance limit. Thus, if the cyclic stress of 795 MPa or less is applied to the steel failure will never occur. S-N curve of high cycle fatigue is composed of the following three parts.

1. The inclined line of finite life region (N_F in logarithmic scale) which shows longer fatigue life N_F with decreasing stress amplitude (σ_a).
2. The minimum number of fatigue cycles N_{knee}=N_2 (knee point) at which fatigue failure does not occur with additional stress cycles.
3. The horizontal line of fatigue limit σ_D below which no fatigue failure occurs.

The estimated S-N curve can be drawn on log-log axes as shown in figure 3.20. S_m is the material strength at 10^3 and difined as $S_m = 0.9\ S_u$ and the corected $S_e \approx 0.5\ S_u$ is ploted at 10^6 cycles, a straight line is drawn between S_m and S_e. The equation of a line from S_m to S_e is the Wohler equation expressed in eq. [3.3].

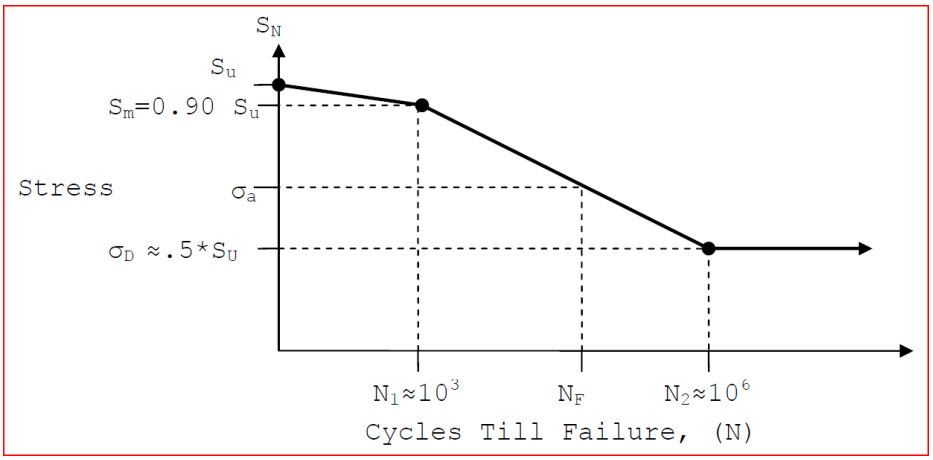

Figure.3.20: estimated S-N curve (Wohler) for steels.

In order to calculate the mean stress (S_m), the estimated S-N Curve for steel depicted in figure 3.20 is considered.

$$S_m = 0.9 * S_u = 0.9 * 1590 \text{ Mpa} = 1431 \text{ Mpa}$$

Adjusted fatigue limit(Modified endurance limit), $S_D = S_e = K_L K_G K_S K_T K_{SR} \acute{S_e} \approx 0.5 * S_u$

where, K_L =load factor, K_{EN} =environmental factor, K_S =size factor, K_T =temperature factor, K_{SR} = surface factor, and $\acute{S_e}$ = endurance limit.

$$S_e = K_L K_G K_S K_T K_R \acute{S_e} \approx 0.5 * S_u = 0.5 * 1590\ Mpa = 795\ Mpa$$

By substituting the value of $S_m$and S_e, the alternating stress (amplitude stress) can be calculated at different values of number of cycles.

$$at, N = 10, \qquad \log_{10}(S) = \frac{1}{3}\log_{10}\left(\frac{795}{1431}\right) * \log_{10}(10) + \log_{10}\left(\frac{(1431)^2}{795}\right) = 3.325$$

$$S = \sigma_a = 10^{3.325} = 2113.48\ Mpa$$

Table 3.9: calculated values for maximum stress and number of cycles from S-N curve.

Number of cycles(N)	Alternating stress of AISI-H13 die steel (MPa)
10	2113.48
100	1740.60
200	1640.6
2000	1349
1000	1431
10000	1176.25
20000	1108.9
100000	966.94
1000000	795
10000000	653

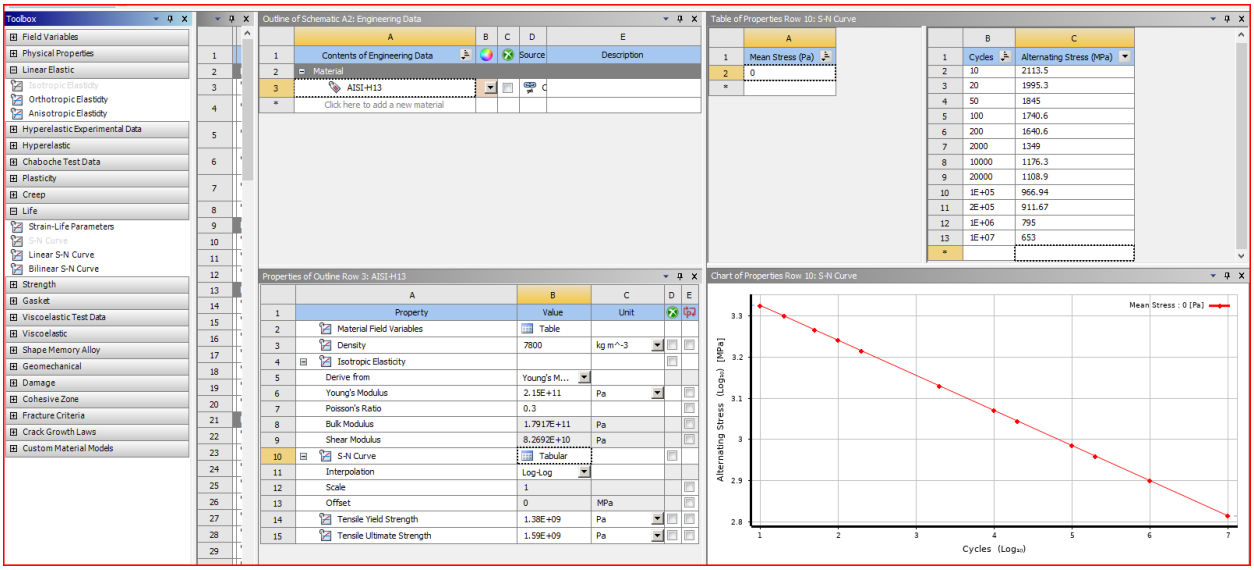

Figure.3.21: S-N curve for AISI-H13 die steel used for pickaxe piercing

CHAPTER4: ANALYTICAL ANALYSIS OF FORGING LOAD

The analytical solution is very important (essential) in designing the open-die forging process for small scale and medium scale industries. The aim of the present study was to develop an analytical model for the forging load during open die forging using rectangular work-piece. The purpose of the analytical method in the open-die forging process is to provide rough and quick estimation of the forging load. In line with the objective, the analytical modeling for rectangular cross-section was derived using an analytical derivation for work-piece with rectangular cross-section. The model used the geometrical features (dimension, shape, material) of the work-piece as input.

In this study, the finite element method-based simulation software (DEFORM-3D) was used to verify the performance of the derived analytical solution. Therefore, this analytical solution is used as a benchmark for validation using numerical methods.

4.1 Methods used for forging load analysis

The primary objective of the mathematical analysis of a forging process is to estimate the forging load. In this study, the two modeling methods, Slab-line method and slip-line field method have been used to analysis the forging load of pickaxe work-piece material. The slab-line method is developed assuming a homogeneous material flow and a constant frictional shear stress during forming. The slip-line field method is used to analyze the pressure under the indentation of a narrow, frictionless punch. This method is more accurate for non-homogeneous deformation.

4.2 Flow stress calculation for work-piece

Flow stress is a function of strain, strain rate and temperature. It was assumed that the flow stress of the workpiece metal is determined by the power law Equation [3.1].Taking the value of Strain-rate sensetivity exponent(m), m=0.105, strength constant(C), C=244 Mpa, from data table 2.2,the flow stress for AISI-1045 is calculated as follow:

$$\sigma_o = C\dot{\varepsilon}^m \qquad [4.1]$$

where, $\dot{\varepsilon}$ =Strain rate $= \frac{d\varepsilon}{dt} = \frac{1}{L} * \frac{dL}{dt} = \frac{V}{h}$ and ε = true strain $= \ln\left(\frac{h_0}{h_1}\right)$

$$V = \frac{\pi NS}{60} * \sin\alpha_N$$

Where, S=Stroke of main ram/constant/=200mm

V=velocity of the ram(mm/s)

N=Revolution of crank shaft=30 rpm

α_N =Nominal crank angle

The triple cranck press PK-300/100 with The rated pressure of 300 tons (2943 KN) was applied over a distance of h=200mm(0.2m). The permissible pressing force is located between 2500 and 3000KN, as it can be identified from figure3.13. Therefore, the crack position above BDC (bottom dead center) is 10^0.i.e $\alpha_N = 10^0$

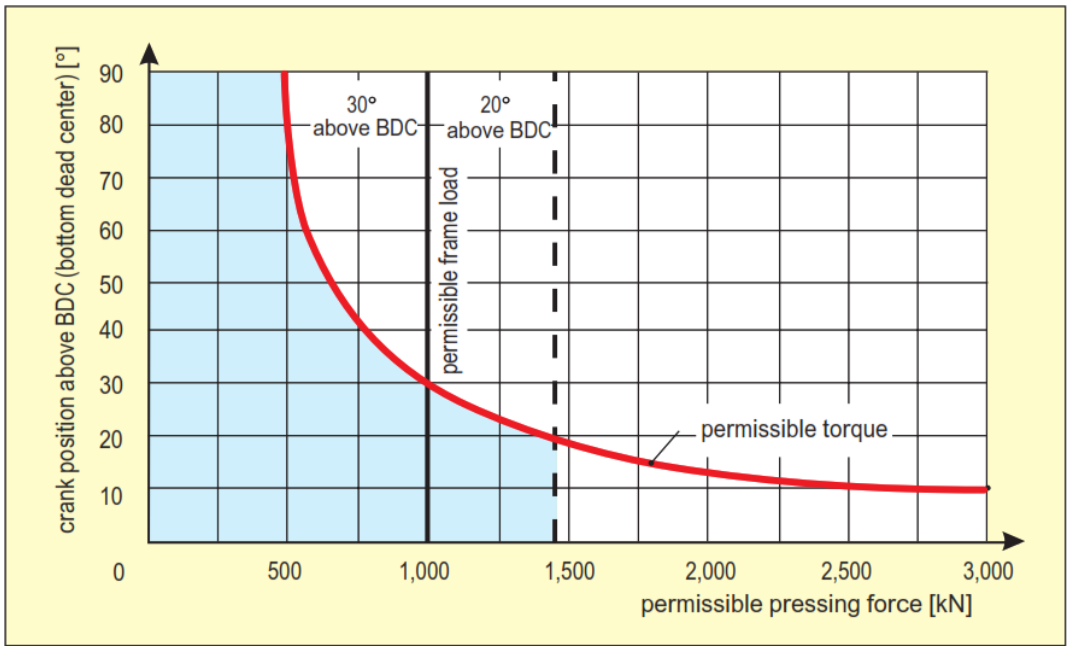

Figure 4.1: Permissible press force and an eccentric press as a function of crank angle[29]

$$V = \text{velocity of the ram}\left(\frac{mm}{s}\right) = \frac{\pi NS}{60} * \sin\alpha = \frac{3.14 * 30 * 200}{60} * \sin 10 \approx 60 mm/s$$

$$\dot{\varepsilon} = \text{Strain rate} = \frac{d\varepsilon}{dt} = \frac{1}{L} * \frac{dL}{dt} = \frac{V}{h} = \frac{60}{41} = 1.46 s^{-1}$$

$$\varepsilon = \text{true strain} = \ln\left(\frac{h_0}{h_1}\right) = \ln\left(\frac{60}{41}\right) = 0.38 \approx 0.4$$

$\sigma_o = C\dot{\varepsilon}^m = 244 * (1.46)^{0.105} = 253.89$ MPa(at 900C and strain of $0.4, C = 244, m = 0.105$)

- at 1000^0C, $\sigma_o = 170.3 * (1.46)^{0.134} = 178.84$ MPa
- at 1100^0C, $\sigma_o = 108.9 * (1.46)^{0.173} = 116.26$MPa
- at 1200^0C, $\sigma_o = 74.5 * (1.46)^{0.188} = 79.99$ MPa

4.3 Calculation for forging load

4.3.1 Indentation load Estimation (slip-line analysis)

Indenting (Piercing) generally implies a blind cavity made by displacement with no removal of metal. It can be used to create a cavity or hole in the work piece. Piercing does not involve breaking through the metal's surface, like a drilling operation. Instead, the hole is pressed into the work-piece, hence it is a forging operation. With the listed assumptions and consideration

1. the material is isotropic and homogeneous
2. the deformation of material is plane strain type
3. constant shear stress at interfaces
4. the material is rigid-idealy plastic(i.e., no strain hardening

Based on upper bound theorem, the total power disipated is given as sum of the power required for internal deformation , shear losses, and friction losses.

$\dot{E} = \dot{W}_{internal} + \dot{W}_{shear} + \dot{W}_{friction}$

$\dot{E} = \int_V \bar{\sigma}\dot{\varepsilon}dV + \int_{S\Gamma} K|\Delta V|dS + \int_{Sf} mK|\Delta V|dS$

$\dot{W}_{internal}$ = rate of energy dissipation for internal deformation

$(= 0,$ no change in volume in dformation process$)$

$\dot{W}_{shear}$ = rate of energy dissipation due to shear losses

$(= 0,$ for continuous velocity field$)$

$\dot{W}_{friction}$ = rate of energy dissipation due to friction losses

Therefore,applying constant friction law,frictional power dissipated along the die surface and the interface of the work-piece can be obtained from the velocity discontinuities. Depending on figure3.14, the Work done can be assumed along the shear force align to direct in AB, BC, AC, and CD.

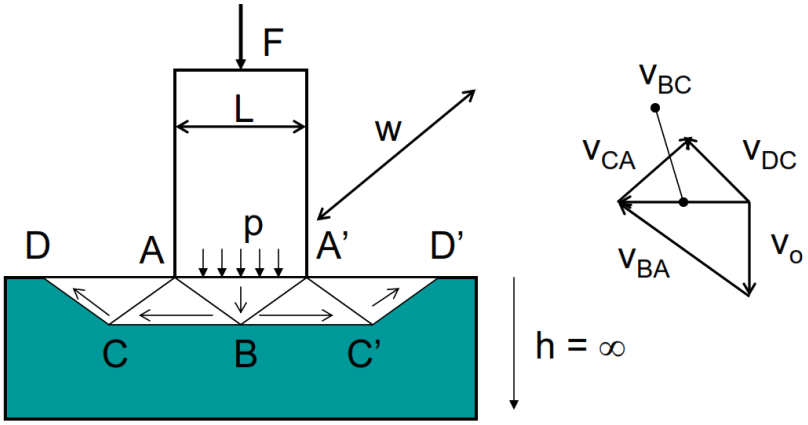

Figure 4.2: schematic diagram of shearing velocity direction in forging process

shearing velocities $V_{BA}, V_{BC}, V_{CA},$ and V_{DC} can be approximated usingV_0(initial velocity of the piercing die).

$$V = \sum \begin{Bmatrix} V_{BA} = V_0\sqrt{2} \\ V_{BC} = V_0 \\ V_{CA} = \frac{V_0}{\sqrt{2}} \\ V_{DC} = \frac{V_0}{\sqrt{2}} \end{Bmatrix}$$

$$\Rightarrow \mathbf{V} = V_{BA} + V_{BC} + V_{CA} + V_{DC}$$

$$\Rightarrow \mathbf{V} = V_0\sqrt{2} + V_0 + \frac{V_0}{\sqrt{2}} + \frac{V_0}{\sqrt{2}}$$

$$\Rightarrow \mathbf{V} = \frac{V_0\sqrt{2}}{\sqrt{2}} + V_0 + \frac{V_0}{2} + \frac{V_0}{2}$$

Where, V=sum of the shearing velocities for$V_{BA}, V_{BC}, V_{CA},$ and V_{DC} to the normal surface. Shearing force along any boundary, per unit length(w=1) is K(shear yield stress) times the length of the boundary, L.

$$\textbf{Total power delivered} = (\textbf{shearing force}) * (\textbf{shearing velocity})$$

$$\dot{E} = F * V \Rightarrow FLV_0 = 2KL * V$$

$$FLV_0 = 2KL * (V_{BA} + V_{BC} + V_{CA} + V_{DC})$$

$$FLV_0 = 2KL\left(\frac{V_0\sqrt{2}}{\sqrt{2}} + V_0 + \frac{V_0}{2} + \frac{V_0}{2}\right) = 6KLV_0$$

$$\text{using } \sigma_{avg} = \frac{F}{A} = P \Rightarrow F = P * A \text{ and } V = A * V_0 = LV_0$$

$$PLV_0 = 6KLV_0 \Rightarrow P = 6K$$

On the rigtht side,each term has been counted twice for symmetry reasons. Due to the complexity of the 3D-geometrical models, the forging process is considered in the plane strain condition (two-dimensional). The non-uniformity in metal flow is not considered. Thus, plane-strain assumes that plane section before the deformation remains plane during deformation. From Von-mise criteria for plane-strain condition:

$$\sigma_1 - \sigma_3 = \frac{2}{\sqrt{3}}\sigma_0 = 2\tau = 2k, \qquad K = \frac{\sigma_0}{\sqrt{3}} = 0.577 * \sigma_0$$

$$\Rightarrow P = 6K = 6 * \frac{\sigma_0}{\sqrt{3}} = 3.46 * \sigma_0$$

but the exact solution is $P = 5.14K = 2.97 * \sigma_0$. so it can be seen the effect of onstraint(redundant work): higher pressure.

Non-homogeneous deformation and Redundant(unwanted deformation) work

If the slab is thick or friction:

- non-homogeneous deformation
- redundant work

If the slab is thin or unconstrained:

(e.g., open die forging without friction)

- no redundant work

Redundant work limit ($\triangle = h/L$)(plane strain)

- $\frac{h}{L} \angle 1$, no redundant work, $p = 1.15 * \sigma_0$
- $1 \leq \frac{h}{L} \leq 8.7$, some redundant work, $1.15 * \sigma_0 \leq p \leq 2.97 * \sigma_0$
- $\frac{h}{L} \geq 8.7$, redundant work $-$ same as infinite plate, $p = 2.97 * \sigma_0$

  In this case, $\frac{h}{L} = \frac{h}{d_{avg}} = \frac{60}{42} = 1.4 \Rightarrow 1 \leq 1.4 \leq 8.7$

Redundat work correction factor(Q_r)

Redundant work correction factor (Q_r) Can be characterized by, $p = Q_r * \sigma_0$.

By using the Tresca yield criterion (maximum shear stress criterion), correction factor for redundant work(Q_r) is expressed by:

$$Q_r = \frac{P}{\sigma_y} = \frac{P}{2\tau_y} \quad \text{from Tresca yield criterion, } \tau_y = \tau_{max} = \frac{1}{2}(\sigma_1 - \sigma_3) = \sigma_o$$

$$(\sigma_1 - \sigma_3) = 2\tau_y = 2\sigma_0 \Rightarrow \sigma_y = 2\tau_y = 2\sigma_o$$

(For plane strain, $\sigma_1 - \sigma_3 = \sigma_1 = \sigma_y, \sigma_3 = \sigma_z = 0$)

$$Q_r = \frac{P}{2\sigma_o}, \qquad \text{where } \sigma_o = \text{The flow strength of the metal} = 253.89 \text{ MPa}$$

$$P = 6K = 3.46 * \sigma_0 = 3.46 * 253.89 \text{ MPa} = 878.46\text{MPa}$$

$$Q_r = \frac{P}{2\sigma_o} = \frac{878.46\text{MPa}}{2 * 253.89} = 1.73$$

$$p = Q_r * \sigma_0 = 1.73 * \sigma_0 = 1.73 * 253.89 = 439.22\text{MPa}$$

$$1.15 * \sigma_0 \leq p \leq 2.97 * \sigma_0 \Rightarrow 291.97 \leq 439.22 \leq 754\text{MPa}$$

According to the redundant work limit criteria ,the piercing(forging) load is within the range ,i. e. some redandant work.

Average Piercing pressure due to punching operation

$$P_{piercing} = P = Q_r * \sigma_0 = 1.73 * \sigma_0$$

$$P_{piercing} = 1.73 * 253.89 = 439.22\text{MPa}$$

4.3.2 Forging load estimation (slab-line method analysis)

The slab analysis method with the assumption of constant frictional shear stress is used as the basis for the forging load calculation equation. The slab method assumes that the metal deforms uniformly in the deformation zone (material flow is homogeneous during forming) [33]. The purpose of the calculation is to find the forging load (F) using the approach of finding pressure distribution p(x) on die surface and integrating it. For an element, equilibrium condition is considered to get a differential equation relating stresses in the variation direction (x,y). To simplify the analysis, the following assumsions have been made :

- the forging force (F) attains its maximum at the end ot forging.
- two-dimensional (plane-strain) cases are considered
- The work piece material behaves like a ideal plastic material

- Elastic deformation and inertial effects are ignored
- The coficient of friction(μ) between the workpiece and the die is constant.
- Internal friction of the material is ignored
- The forged material follows the von-mises falure criteria
- The variation of the stress field along the y-direction is negligible, not considered.

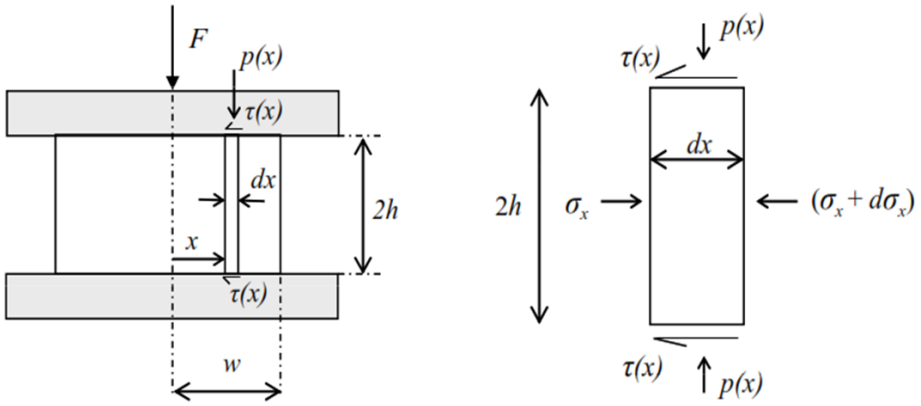

Figure 4.3: schematic diagram of slab method

An element under the die of length (dx) is subjected to a longitudinal stress (σ_x) and a vertical stress(σ_y) due to a die pressure(p).Taking unit depth(D=1) into the diagram, width dx ,and height 2h.

Equilbrium forces in the "X" direction (horizontal).

$$\sum F_x = 0 \Rightarrow (\sigma_x + d\sigma_x) * 2h - (\sigma_x) * 2h - (2\tau_{xy}) * dx = 0$$

$$(d\sigma_x) * 2h = (2\tau_{xy}) * dx \Rightarrow \frac{d\sigma_x}{dx} = \frac{\tau_{xy}}{h}$$

Equilbrium forces in the "y" direction (vertical)

$$\sum F_y = 0 \Rightarrow \sigma_y * dx + P * dx = 0 \Rightarrow \sigma_y = -P$$

Where, P=die pressure, σ_x, σ_y= longitudinal and vertial stress and τ_{xy}=friction force

Assuming a friction law, The usual choices are Coulomb friction (τ =μp), or sticking friction (τ = k, where k is the shear yield stress).

Forging pressurre due to sticking condition (sticking friction (τ = k)

$$P_{sticking} = P_{avg} = Y * \left[1 + \frac{a}{2h}\right] = \frac{2}{\sqrt{3}}\sigma_0 * \left[1 + \frac{a}{2h}\right]$$

$$P_{sticking} = \frac{2}{\sqrt{3}} * 253.89 * \left[1 + \frac{15}{2 * 41}\right] = 346.8\ \text{MPa}$$

Forging pressurre due to sliding condition(Coulomb friction, τ =μp)

$$P_{avg} = Y * \left[1 + \frac{\mu a}{h}\right] = \frac{2}{\sqrt{3}}\sigma_0 * \left[1 + \frac{\mu a}{h}\right]$$

$$P_{avg} = \frac{2}{\sqrt{3}} * 253.89 * \left[1 + \frac{0.7 * 15}{31}\right] = 392.46\text{MPa}$$

Total Forging pressurre due to piercing , sticking, and sliding condition

$$P_{total} = \left(P_{piercing} + P_{sticking} + P_{sliding}\right) = 439.22 + 346.8 + 392.46 = 1178.46\ \text{MPa}$$

Total Forging load due to piercing, sticking , and sliding condition

Total forging load = (total average forging pressure) * (area at the end of forging)

$$F_{total} = P_{total} * A$$

P_{total} = total average forging pressure = $\left(P_{piercing} + P_{sticking} + P_{sliding}\right) = 1178.46$ MPa

A = area at the end of forging = projected area of forged workpiece on lower die

$$A = A_{\text{rectangular part}} + A_{\text{circular part}} = w * L + \pi * \frac{d^2}{4}$$

$$A = w * L + \pi * \frac{d^2}{4} = 0.03 * 0.042 + \pi * \frac{(0.058)^2}{4} = 3.9 * 10^{-3}\text{m}^2$$

$$F_{total} = \left(P_{piercing} + P_{sticking} + P_{sliding}\right) * \left(w * L + \pi * \frac{d^2}{4}\right)$$

$$F_{total} = (1178.46 * 10^6\text{Pa}) * (3.9 * 10^{-3}\text{m}^2) = 4595994\text{N}$$

$$F_{total} = \frac{4595994\text{N}}{9.81 * 1000} = 468.5\text{ton}$$

Average sticking pressure at different value of flow stress(σ_o)

$$P_{sticking} = P_{avg} = \frac{2}{\sqrt{3}}\sigma_0 * \left[1 + \frac{a}{2h}\right] = \frac{2}{\sqrt{3}}\sigma_0 * \left[1 + \frac{15}{2 * 41}\right] = 1.366\sigma_0$$

At $\sigma_o = 253.89$, $P_{sticking} = 1.366\sigma_0 = 1.366 * 253.89 = 346.8$ MPa

At $\sigma_o = 178.84$, $P_{sticking} = 1.366\sigma_0 = 1.366 * 178.84 = 244.29$ MPa

At $\sigma_o = 116.26$, $P_{sticking} = 1.366\sigma_0 = 1.366 * 116.26 = 158.8$ MPa

At $\sigma_o = 79.99$, $P_{sticking} = 1.366\sigma_0 = 1.366 * 79.99 = 109.26$ MPa

Average sliding pressure at different value of flow stress(σ_o)

$$P_{avg} = Y * \left[1 + \frac{\mu a}{h}\right] = \frac{2}{\sqrt{3}}\sigma_0 * \left[1 + \frac{0.7 * 15}{31}\right] = 1.5458\sigma_0$$

At $\sigma_o = 253.89$, $P_{sliding} = 1.5458\sigma_0 = 1.5458 * 253.89 = 392.4$ MPa

At $\sigma_o = 178.84$, $P_{sliding} = 1.5458\sigma_0 = 1.5458 * 178.84 = 276.45$ MPa

At $\sigma_o = 116.26$, $P_{sliding} = 1.5458\sigma_0 = 1.5458 * 116.26 = 179.7$MPa

At $\sigma_o = 79.99$, $P_{sliding} = 1.5458\sigma_0 = 1.5458 * 79.99 = 123.6$ MPa

Piercing pressure at different value of flow stress(σ_o)

$P_{piercing} = P = Q_r * \sigma_0 = 1.73 * \sigma_0$

At $\sigma_o = 253.89$, $P_{piercing} = 1.73 * \sigma_0 = 1.73 * 253.89 = 436.22$ MPa

At $\sigma_o = 178.84$, $P_{piercing} = 1.73 * \sigma_0 = 1.73 * 178.84 = 309.4$ MPa

At $\sigma_o = 116.26$, $P_{piercing} = 1.73 * \sigma_0 = 1.73 * 116.26 = 201$ MPa

At $\sigma_o = 79.99$, $P_{piercing} = 1.73 * \sigma_0 = 1.73 * 79.99 = 138.38$ MPa

Total forging load at different value of flow stress(σ_o)

$F_{total} = P_{total} * A = (P_{piercing} + P_{sticking} + P_{sliding}) * A$

At $\sigma_o = 253.89$, $F_{total} = P_{total} * A = 1178.46 * (3.9 * 10^{-3} m^2) = 4595994N = 468.5$ ton

At $\sigma_o = 253.89$, $F_{total} = P_{total} * A = 830 * (3.9 * 10^{-3} m^2) = 3237546N = 330$ ton

At $\sigma_o = 253.89$, $F_{total} = P_{total} * A = 539.5 * (3.9 * 10^{-3} m^2) = 2104050N = 214.48$ ton

At $\sigma_o = 253.89$, $F_{total} = P_{total} * A = 371.24 * (3.9 * 10^{-3} m^2) = 1447836N = 147.58$ ton

Table 4.1: Summary of flow stress, forging pressure and forging load for pickaxe piercing die at different temperature and with coefficient of friction=0.7

Temperature(^{0}C)	Flowstress (σ_0) (MPa)	Forging pressure (MPa)	Forging load N(ton)
900	253.89	1178.46	4595994 (468.5)
1000	178.84	830	3237546 (330)
1100	116.26	539.5	2104050 (214.48)
1200	79.99	371.24	1447836(147.58)

Table 4.2 Summary of stress, forging pressure and forging load for pickaxe piercing die at different temperature and with coefficient of friction=0.5

Temperature (^{0}C)	Flowstress (σ_0) (MPa)	Forging pressure (MPa)	Forging load N(ton)
900	253.89	1178.46	4473378 (456)
1000	178.84	830	3159546 (322)
1100	116.26	539.5	2053350 (209)
1200	79.99	371.24	1413126(144)

Table 4.3: Summary of flow stress, forging pressure and forging load for pickaxe piercing die at different temperature and with coefficient of friction=0.3.

Temperature(^{0}C)	Flowstress (σ_0) (MPa)	Forging pressure (MPa)	Forging load N(ton)
900	253.89	1178.46	4363008 (444.75)
1000	178.84	830	3081663 (314)
1100	116.26	539.5	2002767 (204)
1200	79.99	371.24	1378299(140.4)

CHAPTER 5: RESULTS AND DISCUSSIONS

5.1 Response of Simulation

In order to quantify the forging load on the die, three-dimensional material flow simulations are first carried out using FEM. The forging process was simulated and the forging load was calculated using DEFORM-3D software. Using Taguchi's experimental design method, a series of analysis were carried out to find the minimum forging load by changing the work-piece and die temperature, and the coefficient of friction between the die and work-piece.

5.2 Optimization and forging process parameters

The full factorial method i.e., Taguchi's method was used to identify the best combination of factors to achieve the objective and to find the influence of each parameter on the result of the experiment. The objective of conducting the Taguchi experiment was to predict the optimum forging load and select the appropriate forging process parameters (factors). In this study, there are three factors and three levels of each factor. These factors were work-piece temperature (900, 1000, 1050C), die temperature (150,200,250C), and coefficient of friction (0.3, 0.5, 0.7). According to the L27 Orthogonal Array, 27 experiments were conducted using the DEFORM-3D simulation software. The response obtained from this simulation software was a forging load. The forging load obtained during 27 experiments was recorded and is shown in table 5.1. After obtaining the simulation results, the full factorial Taguchi problem was solved using MINITAB 22 software. This statistical software showed the best optimal combination and contribution of each parameter to the forging load. To minimize the response parameter (forging load), a large signal-to-noise ratio (-46.8485) was considered.

Table 5.1: Simulation result for forging loads and the corresponding S/N ratios

Simulation Run	Simulation control factors			Response parameter	S/N ratios for Forging load
	Work-piece Temp.(^{0}C)	die Temp.(^{0}C)	Friction coefficient(μ)	Forging Load MN/ton	
R1	900	150	0.3	3.26/332	-50.4228

Table 5.1 continued

R2	900	150	0.5	4.11/418.96	-52.4435
R3	900	150	0.7	4.47/455.6	-53.1717
R4	900	200	0.3	3.24/330	-50.3703
R5	900	200	0.5	3.89/396.5	-51.9649
R6	900	200	0.7	4.4/448.5	-53.0352
R7	900	250	0.3	3.19/325	-50.2377
R8	900	250	0.5	3.8/387.4	-51.7632
R9	900	250	0.7	4.38/446.4	-52.9945
R10	1000	150	0.3	2.57/260.9	-48.3295
R11	1000	150	0.5	3.07/311.9	-49.8803
R12	1000	150	0.7	3.58/364.9	-51.2435
R13	1000	200	0.3	2.52/256.8	-48.1919
R14	1000	200	0.5	3.06/312.9	-49.9081
R15	1000	200	0.7	3.59/365.9	-51.2672
R16	1000	250	0.3	2.51/255.86	-48.1600
R17	1000	250	0.5	3/305.8	-49.7087
R18	1000	250	0.7	3.33/339.4	-50.6142
R19	1050	150	0.3	2.32/236.4	-47.4729
R20	1050	150	0.5	2.77/282	-49.0050
R21	1050	150	0.7	2.99/304.8	-49.6803
R22	1050	200	0.3	2.2/224	-47.0050
R23	1050	200	0.5	2.68/273	-48.7233
R24	1050	200	0.7	2.92/298.6	-49.5018
R25	1050	250	0.3	2.16/220	-46.8485
R26	1050	250	0.5	2.57/261.9	-48.3627.
R27	1050	250	0.7	2.86/291.5	-49.2928

5.2.1 Response table of signal to noise ratios for forging load

The signal to noise ratio response table indicates the rank of each parameter. The work-piece temperature (rank-1) was found to have a greater influence on forging load, followed by

coefficient of friction (rank-2) and die temperature (rank-3). The main effect plot for the signal to noise ratio of three forging factors is shown in Figure 5. The decrease in forging load was observed at a higher level of forging factors. Table 5.2 shows the optimal level value for each factor. The values in bold are the largest values of the S/N ratios.

Table 5.2: signal to noise ratios Response table

level	Work-piece temperature(°C)	Die Temperature(°C)	Coefficient of friction(μ)
1	-52.82	-50.18	**-48.56**
2	-49.70	-50.00	-50.20
3	**-48.43**	**-49.78**	-51.20
delta	3.39	0.41	2.64
rank	1	3	2
Smaller is better			

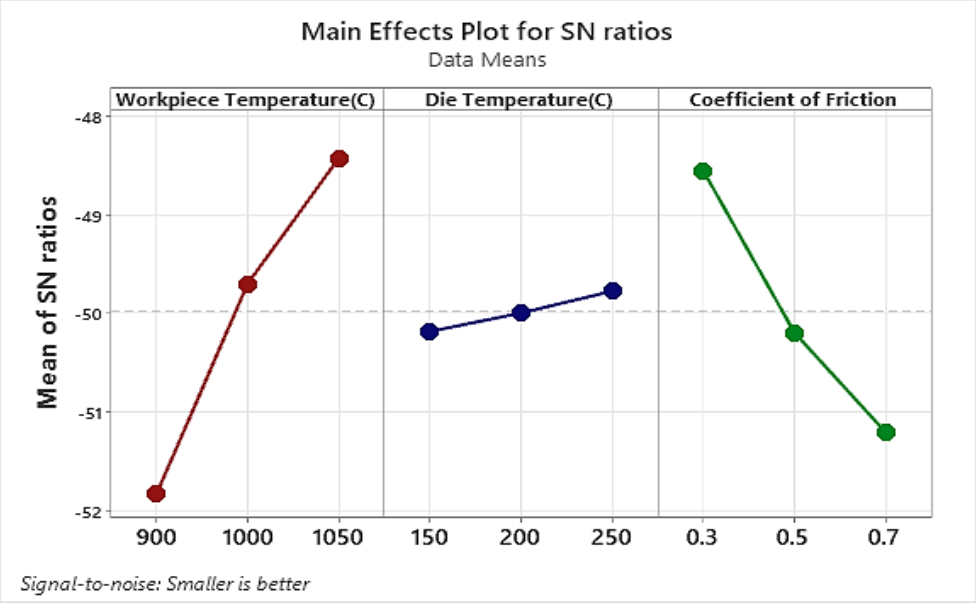

Figure 5.1: Main affects plots for S/N ratios of the applied forging load

The graphical representation of the S/N ratio in Figure 5.1 shows that the combination of 1050,250 and 0.3 is the best combination to achieve the smallest forging load.

5.3 Regression Analysis and Analysis of variance (ANOVA)

5.3.1 Regression Analysis of the minimum forging load

To investigate the relationship between the dependent (forging load) and independent variables (forging process parameters), regression analysis was used in this study. The dependent factor in this study is the minimum forging load, whereas the independent factors are the work-piece temperature, die temperature, and coefficient of friction. The developed regression model is based on a regression analysis for the response and is given in an equation in terms of the work-piece temperature (Tw=1050C), die temperature (Td=250C), and the coefficient of friction (μ=0.3). The predicted equation from the linear regression analysis for the minimum forging load is presented as:

$$Forging\ load(ton) = 1067.2 - 0.8506 * Tw - 0.1491 * Td + 243.0 * \mu = 209.69 \approx 210$$

$$\text{Percentage error} = \frac{\text{simulation value}(220) - \text{predicted value}(210)}{\text{simulation value}(220)} * 100 = 4.68\%$$

The percentage error, among virtual simulation experiment and optimization (predicted) result was found to be within the acceptable limit (i.e., 4.68<5%).

5.3.2 Analysis of variance (ANOVA)

The purpose of ANOVA is to investigate which forging process parameters significantly affect the forging process. The experimental data (test data) was analyzed using the MINTAB software, which is specially used for test planning. In order to find out the significant effect of the forging process parameters such as work-piece temperature, die temperature, coefficient of friction, and their interaction on the forging process, ANOVA was carried out using experimental data. Table 4.3 shows that work-piece temperature was identified as the most significant factor affecting forging load, with the highest percentage contribution of 61.33%. This implies that the work-piece temperature plays a key role during deformation, whereas the coefficient of friction and die temperature have a percentage contribution of 0.87% and 37.12%, respectively. Next to the work-piece temperature, the coefficient of friction had the higher percentage contribution and affects (increases the forging loads) the forging load, resulting in inhomogeneous metal flow behavior. The die temperature has the lowest percentage contribution (p-value >0.05). DF stands

for degree of freedom, AdjSS stands for adjusted sum of squares, AdjMS stands for adjusted mean squares, F-value refers to variance ratio, and the P-value refers to probability value (p-value <0.05 is significant and a p-value >0.05 is not significant). The effect is weaker at smaller values of adj MS. Sum of squares (SS) is obtained by summing the squares of the differences between each data value and the overall mean. The F- score for independent groups is calculated from the Mean Squares. The degree of freedom (DF) refers to the number of independent measurements (factors) used in calculating a sum of squares.

$$\text{Sum of Squares} = SS_{total} = SS_{Beetween\ Groups} + SS_{Within\ Groups(error)} = 86.1096$$

$$\text{DF} = \text{DF}_{Beetween\ Groups} = number\ of\ groups - 1 = 3 - 1 = 2$$

$$\text{DF} = \text{DF}_{Within\ Groups(error)} = total\ number\ of factors\ in\ each\ groups - 1 = 9 - 1 = 8$$

$$\text{F} = SS_{total} = Mean\ Squares(MS)_{Beetween\ Groups}/Mean\ Squares(MS)_{Within\ Groups(error)}$$

$$Mean\ Squares(MS)_{Beetween\ Groups} = SS_{Beetween\ Groups}/\text{DF}_{Beetween\ Groups}$$

$$Mean\ Squares(MS)_{Within\ Groups(error)} = SS_{Within\ Groups(error)}/\text{DF}_{Within\ Groups(error)}$$

Table 5.3: Forging process parameters percentage contribution

source	DF	AdjSS	AdjMS	F	P	Contribution %
A	2	52.8141	26.4070	1041.66	0.000	61.33%
B	2	0.7488	0.3744	14.77	0.002	0.87%
C	2	31.9678	15.9839	630.51	0.000	37.12%
A*B	4	0.0878	0.0219	0.87	0.524	0.102%
A*C	4	0.1978	0.0497	1.96	0.194	0.23%
B*C	4	0.0477	0.0119	0.47	0.756	0.055%
Error	8	0.2028	0.0254			0.00235
total	26	86.1096	42.8742			99.88≈100%

5.4 Forging process simulation after optimization

Figure 4.25 - 4.27 shows the forging simulation result obtained after using the optimal forging process parameters from Figure 4.24 and Table 4.13. The flow characteristics of the metal are sensitive to forging parameters such as work-piece temperature, die temperature, and friction coefficient. By increasing the forging temperature of the work-piece, the flow stress of the work-piece is reduced, so minimizing the required forging load and making the stresses induced in die low. This increases lifespan of the die.

5.4.1 Forging load result

Figure 5.2 shows the result of the optimized forging load. The value was 2.16 MN. The magnitude of the forging load varied with the stroke length (vertical distance of the upper die from the initial position to the final position of the forging stage). As can be seen in figure5.2, the forging load is increased progressively. From this one could conclude that forging load and stroke length have direct relationship. Therefore, the stroke length is considered as a forging parameter.

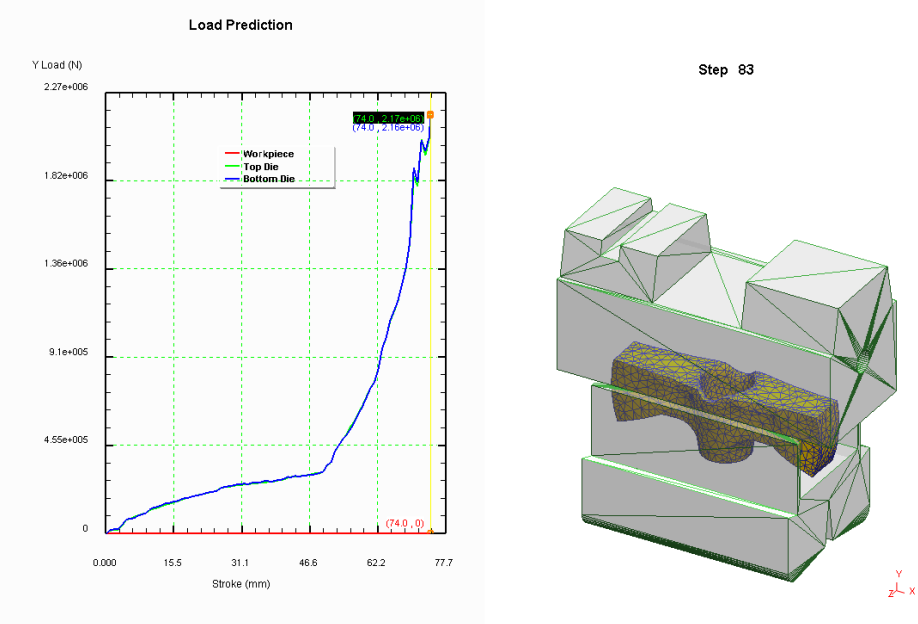

Figure 5.2: The last stage of forging load.

5.4.2 Maximum effective stress result

The maximum effective stress on the work-piece at 1050 is 389 MP from Figue4.3. At room temperature, the Tensile strength is 560 MP and the yield stress is 275 MP. The effective stress of the work-piece at 1050 ^{o}C is greater than the yield stress (389> 275). This implies that the work-piece is plastically deformed. On the other hand, the effective stress of the work-piece at 1050 ^{o}C is lower than the ultimate tensile strength (389<560). This means that the flow stress on the work-piece is reduced during the forging operation is decreased. i.e., could be easily deformed without mechanical damage.

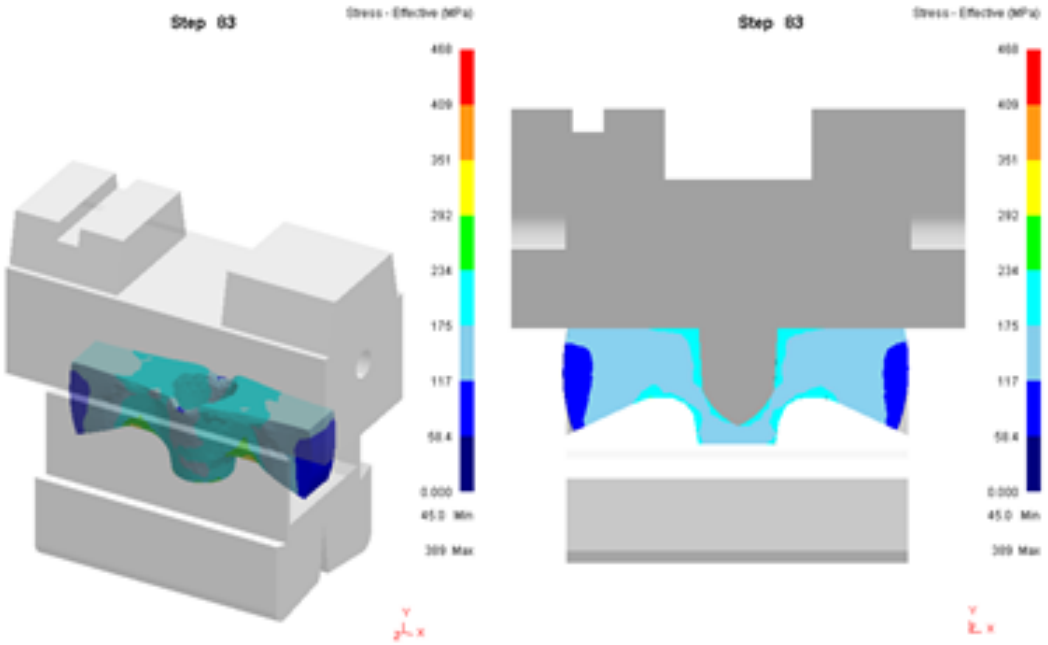

Figure 5.3: Effective stress distribution for the pickaxe work-piece

5.4.3 Maximum principal stress result

The maximum principal stress (326Mpa) is less than the ultimate tensile stress; Therefore, the stress due to reaction force on the lower die is decreased.

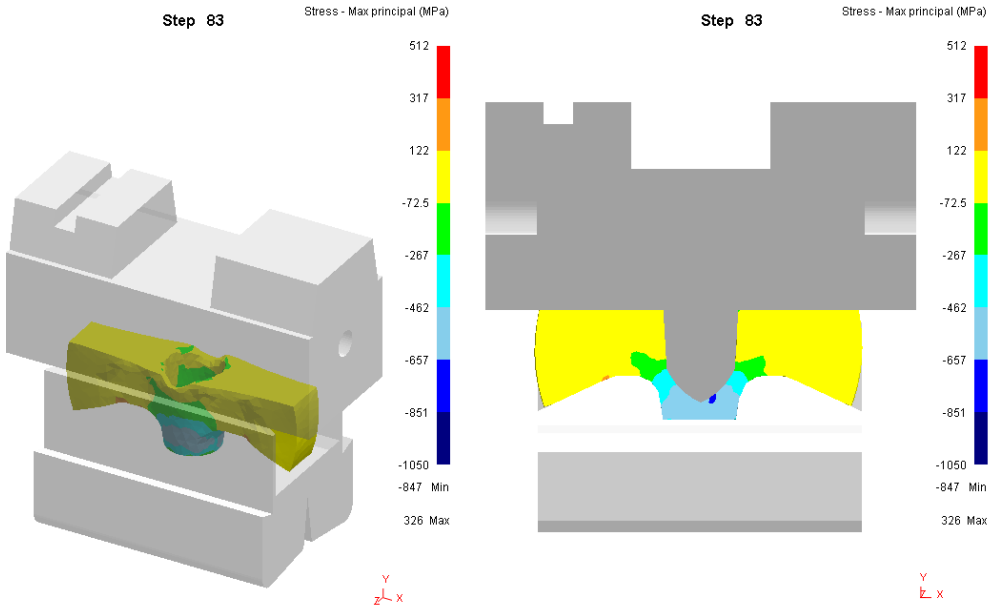

Figure 5.4: Maximum principal stress distribution for the work-piece

5.5 Fatigue life of the lower pickaxe die

This study deals with constant amplitude loading conditions based on the S-N method. The lower pickaxe piercing die is isolated from the assembly set to conduct static and fatigue analysis. The boundary and loading conditions such as magnitude and direction of the loads as well as the location of constraints in the model are shown in Figure 3.21. An S-N curve is plot of the magnitude of an alternating stress relative to the number of cycles until failure of a material. The fatigue analysis of the reference material model in this study is based on the S-N method[13]. The S-N curve for the model is shown in Fig 5.6. Similar material properties, S-N curve data and maximum number of cycles are used in the present study to correlate with the Wohler model.

5.5.1 Equivalent (von-misses) stress result

The main variables to consider in die stress simulation are the effective stress and the maximum principal stress. The effective stress is used to determine whether plastic deformation has occurred at a location on the die. If an effective stress occurs in an area of the die close to or exceeding the yield stress of the die material, that region is at risk of plastic deformation. In this work,the simulation result of the equivalent(effective stress) is 1261.7 Mpa,which is less than the yield stress of the lower die material(1380Mpa). This means that there is no elastic deformation in the die,thereby avoiding dimensional error in the geometry of the forged workiece.

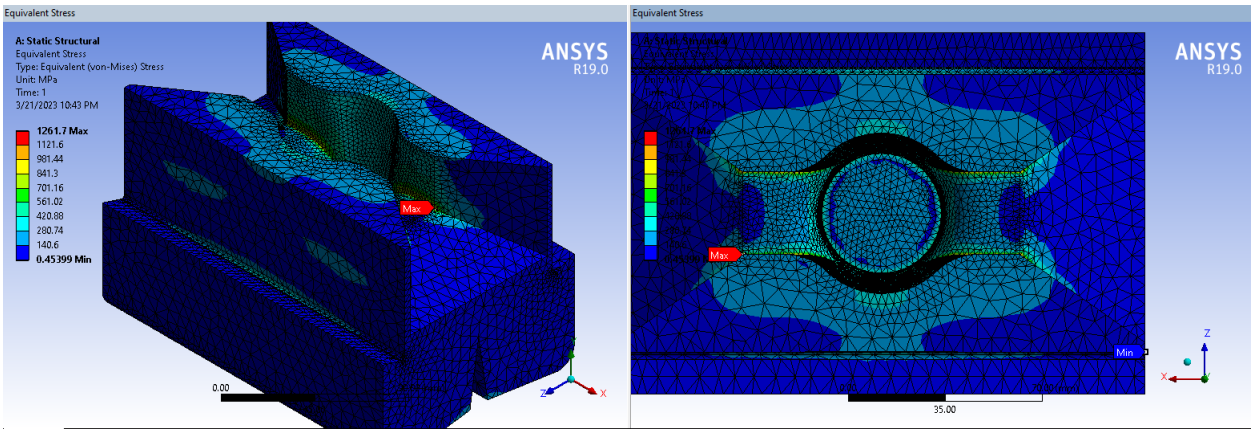

Figure 5.5: Effective stress distribution for the lower pickaxe piercing die

5.5.2 Maximum principal stress result

The maximum principal stress shows wchich regions of the die are in a state of compression and which are in a state of tension. The maximum principal stress is extremely important in

determining whether a die will experience pre-matured failure due to fatigue. The die stress distribution in the die corresponding to the highest load in a forging cycle is shown in Figure 3.6. As can be seen from the maximum principal stress contour, the sides of the grooves are exposed to the compressive stress. This could promote the crack intiation of the die. Thus,working at low forging temperature and high (dry) friction coefficient can be the cause of catastrophic (fracture) failure in hot forging pickaxe die.

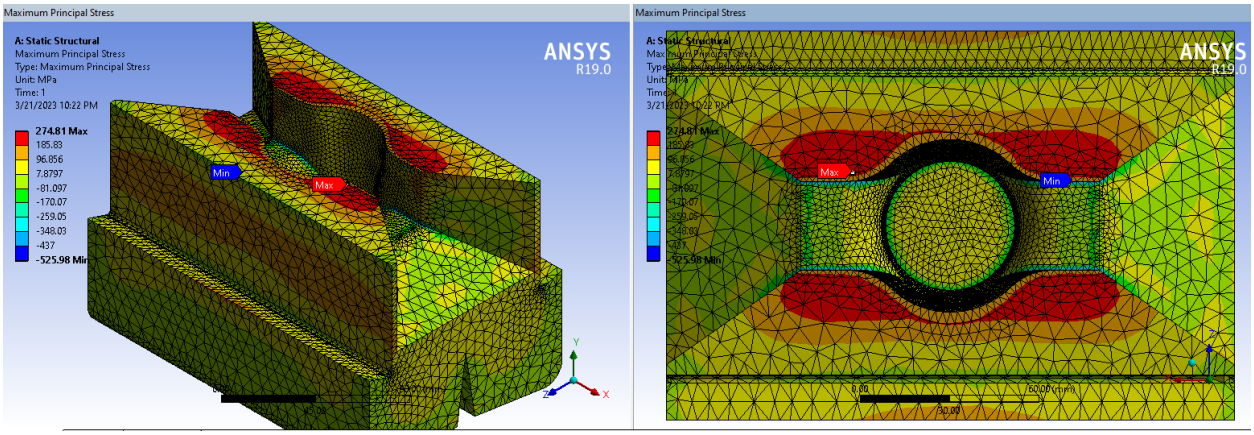

Figure 5.6: Maximum principal stress distribution for the lower pickaxe piercing die

5.5.3 Fatigue Life result

The possible fatigue life for the lower pickaxe piercing die is shown in the fatigue result contour plot. The die may fail after a certain number of cycles because of cracks or other damage will develop due to the cycling load of the forging recess. When the die is subjected to a higher forging load, greater than 2.16 MN, the number of cycles to failure is less.

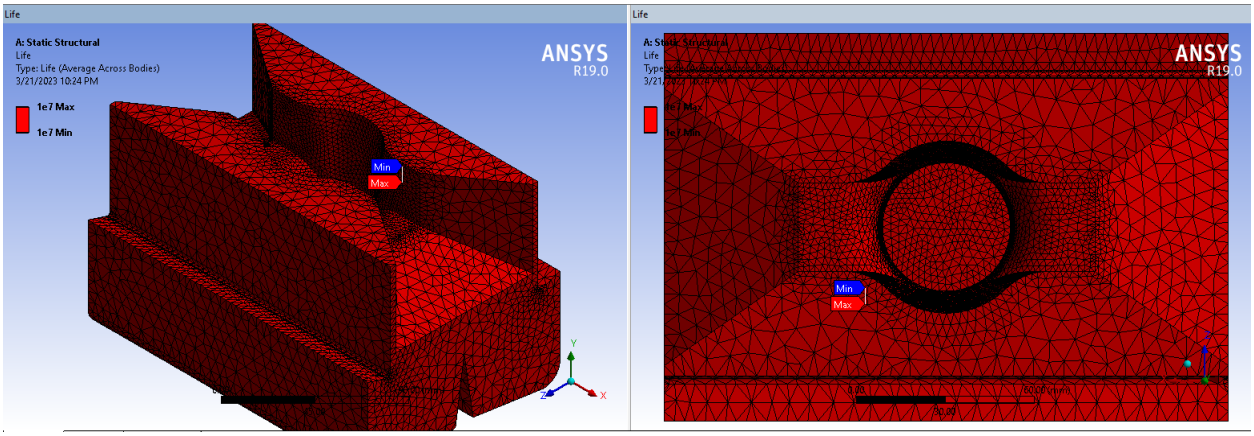

Figure 5.7: Fatigue life analysis result for lower pickaxe piercing die

5.5.4 Safety factor result

The fatigue safety factor is the contour plot of the factor of safety with respect to a fatigue failure at a given design life. The maximum safety factor for this die displayed in Figure is 15. A fatigue safety factor of less than one indicates failure before the design life is reached. For this study, the result is 1.471, which is greater than one. This shows that the die can be maintained in the current forging condition (loading condition) until the design life cycle.

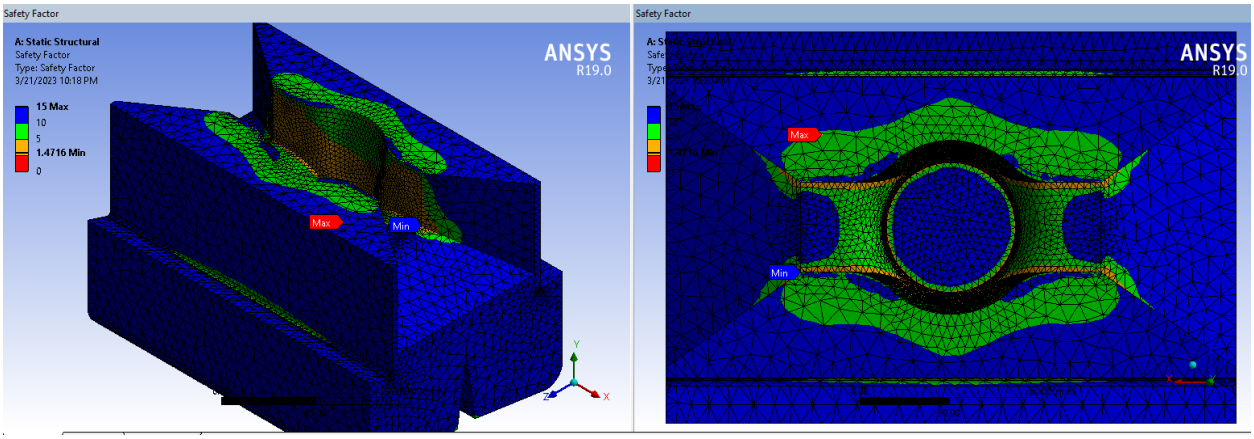

Figure 5.8: Safety factor analysis result for lower pickaxe piercing die

5.6 Impacts of forging process parameters on the die life

The fatigue life and die fatigue stress corresponding to the forging load in a forging cycle are shown in Table 5.4. The results show that increasing the forging temerature and decreaseasing cofficient of friction lead to a reduction in the forging load, thus increasing the fatigue life of the die. The fatigue life of the die is improved by increasing the forging temperature above

1050ºC and redusing the coefficieint of friction below 0.3. Low cycle fatigue (LCF) in this hot forging die is defined by a reduced number of cycles to failure (typically less than 10,000 cycles). As observed in the table, the fatigue life of the die is 0 at work-piece tempppprature of 900 ºC , cofficient of friction of 0.7 and at all die temperatures.

Table 5.4: Fatigue life analysis result for the lower pickaxe forging die

S.Run	Work-piece Tmp (^{0}C)	Die Tmp (^{0}C)	Coefficient of friction(μ)	Forging Load (MN)	Equivalent stress (MPa)	Max.stress MPa	Safety factor	Fatigue Life (cycle)
R1	900	150	0.3	3.26	1904.3	414.76	0.975	1.6e5
R2	900	150	0.5	4.11	2400.8	522.9	0.773	1.35e4
R3	900	150	0.7	4.47	2611	568.7	0.711	0
R4	900	200	0.3	3.24	1892.6	412.2	0.981	1.62e5
R5	900	200	0.5	3.89	2272.3	494.9	0.817	5.2e4
R6	900	200	0.7	4.40	2570.2	559.8	0.722	0
R7	900	250	0.3	3.19	1863.4	405.8	0.996	1.62e5
R8	900	250	0.5	3.80	2219.7	483.5	0.836	9.28e4
R9	900	250	0.7	4.38	2558.5	557.3	0.725	0
R10	1000	150	0.3	2.57	1501.2	326.7	1.236	1e7
R11	1000	150	0.5	3.07	1793.3	390.6	1.035	1e7
R12	1000	150	0.7	3.58	2091.2	455.5	0.887	1.62e5
R13	1000	200	0.3	2.52	1472.	320.6	1.261	1e7
R14	1000	200	0.5	3.06	1787.4	389.3	1.038	1e7
R15	1000	200	0.7	3.59	2097	456.7	0.885	1.62e5
R16	1000	250	0.3	2.51	1466.2	319.3	1.266	1e7
R17	1000	250	0.5	3.00	1752.4	381.7	1.059	1e7
R18	1000	250	0.7	3.33	1945.2	423.6	0.954	1.62e5
R19	1050	150	0.3	2.32	1939.3	422.4	0.957	1.62e5
R20	1050	150	0.5	2.77	1618	352.4	1.147	1e7
R21	1050	150	0.7	2.99	1746.6	380.4	1.063	1e7
R22	1050	200	0.3	2.20	1285.1	279.9	1.445	1e7
R23	1050	200	0.5	2.68	1565.5	340.9	1.186	1e7
R24	1050	200	0.7	2.92	1705.7	371.5	1.088	1e7
R25	1050	250	0.3	2.16	1261.7	274.8	1.471	1e7
R26	1050	250	0.5	2.57	1501.2	326.9	1.236	1e7
R27	1050	250	0.7	2.86	1670.6	363.8	1.111	1e7

CHAPTER 6: CONCLUSION, RECOMMENDATION AND FUTUTE WORK

Conclusion

The objective of this research is to optimize the forging load and investigate the fatigue life of the lower pickaxe die. In order to achieve this objective, the study combined numerical simulation methods and analytical analysis methods to simulate and predict the forging load in upsetting work-piece material. The two proposed methods are used to predict the forging load without the need for experiments. To obtain the results, the forging process was carried out using DORM-3D simulation software at constant flash thickness(10mm) and compared and validated with the analytical method. From the observation of obtained result, the following conclusions have been derived:

From the comparison (validation) of the mathematical model with that of the finite element method, it can be seen that the mathematical model result for rectangular work-piece at all forging temperatures of 900 ^{0}C and dry frictions of 0.7 is higher than the numerical simulation result. Hot forging is non-steady-state type process because metal flow, stresses and temperatures change frequently during the forging process. However, the analytical method considers the forging process as a steady state and does not consider the effect of the priheating temperature of the die. For these reasons, it was difficult to accurately determine the forging load of the work-piece using analytical methods. On the other hand, at 1000-1200^{0}C, the numerical simulation resut is higher than the result of the analytical method because heat loss occurs between the work-piece and the die interface with the environmet. Due to the heat loss, some amount of temprerature is reduced and leads an increase in the flow stress of the work-piece during the forging operation.

The proposed analytical solution is agreed to numerical simulations results, which have an average error of 0.55%. The error was calculated using the ratio of the difference between analytical and simulated results to the analytical result. The proposed simulation process can assist in optimizing different forging process parameters. Furthermore, the proposed methodology can be considered as the one that allows the designer to address the solution for the selection of die material.

In this study, the optimization process is carried out using Taguchi optimization technique which is based on analysis of Variance (ANOVA) to obtain the desired optimum forging load. The three forging process parameters (factors) were work-piece temperature, die temperature and coefficient of friction. Among the three forging process parameters, work-piece temperature is the most significant parameter followed by coefficients of friction and die temperature. The work-piece temperature had the highest percentage contribution at 61.33%, the coefficient of friction had the higher percentage contribution at 37.12%, and the die temperature had the lowest percentage contribution to the forging load next to coefficient of friction. At higher values of the coefficient of friction, the deformation forces increase due to the inhomogeneous metal flow and filling the die becomes more difficult.Therefore, the use of lubricant minimizes friction and reduces barelling effect. The optimal levels (value) of the forging process parameters that must be maintained (controlled) during the forging process in order to reduce the forging load, are 1050^0C for the work-piece temperature, 250^0C for the die temperature, and 0.3 for the coefficients of friction.

To investigate the relationship between the dependent (forging load) and independent variables (forging process parameters), regression analysis was used in this study. A linear regression model was used to predict the dependent factor. The regression analysis result for the forging load was 210 tons and was validated (compared) with the simulation result for the required 220-tons of forging load obtained by test R25 of Taguchi method. The percentage error was 4.68%.

In this study, the forging capacity of the crank press machine is 300 tons. With dry friction at a coefficient of friction of 0.5, a work-piece temperature of 1050C, and a die temperature of 200C, the forging load was 273 tons. And with a coefficient of friction of 0.7, the forging load at the same work-piece and die temperature was 298.6 tons. Thus, the estimated forging loads are less than the forging load of the crank press. The minimum preheating temperature of the die and work-piece should be maintained at 200^0C and 1050^0C respectively. Therefore, in order to extend the life of the die and reduce the die stress due to the reaction force, the parameters of the forging process should be optimized to reduce the flow stress of the work-piece. The investigation of fatigue life is performed based on the finite element analysis(using ANSYS work bench) considering the maximum forging load at the end of the forging stages and assuming the static loading condition. Constant amplitude was used to predict the fatigue life of

the lower die. This study will help to give manufacturer and user with information to improve die fatigue life. In my opinion, this proposed die life prediction model is practical and can be very effective for developing open hot forging die designs and for limiting and maintaining the optimized forging process parameters during the forging operation. By implementing the minimum optimized forging load(2.16 MN), the number of fatigue lives before die failure can be extended to 1million cycles. From the optimization point of view,numerical method is a very useful tool.

Recommendation

The hot forging process needs special attention because it has high importance among manufacturing process, involves mechanical and thermal load , and due to the complicated nature of non-linear physical and material properties present during the forging process.Based on these facts, the finite element simulation must be applied in modelling the forging process to predict the limits of the forging process parameter. This is used to increase the die service life and improve the part (final product quality by avoiding internal surface defects). From the experience of industrial surveys,individuals tried to estimate the forging process parameters such as forging temerature usually with out measuring instruments (thermometers) and used an open furnace instead of a closed furnace to heat the work-piece. These practices contributed to forging die overload and the production of poor quality forgings. Therefore, using quantified (measured) data to accurately estimate the forging load is essential to improve the performance of the forging process.

Future work

From the fatigue life investigations and optimation of forging process parameters, it was observed that the forging force required to forge the work piece was high at lower forging temperature and dry coefficient of friction. Therefore, it could be the cause of die overload; finally, catastrophic failure (fracture) can occur during the forging process. However, in hot forging process, thermal load is the second significant parameter of the forging process, which results from cyclic heating and cooling of the die surface at different forging temperature during the forging operation. Therefore, based on this problem, the investigation of the thermal fatigue life could be the next research focus for this understudied pickaxe forging die.

REFERENCE

1. Akshay S Nandalgaonkar, S.C.B., *Design and Analysis of Forging Die Towards Improving Life of Closed Die By Using Finite Element Analysis.* Ijariie, 2021. **7**(2).
2. S., N.C.A.B., *The Knowledge Based System For Forging Process Design Based On Case-Based Reasoning And Finite Element Method.* Aijstpme, 2012. **5**(2): P. 45-54.
3. Markus J. Ottersböck, Martin Leitner and M.S.A.W.M., *Crack Initiation And Propagation Fatigue Life of Ultra High-Strength Steel Butt Joints.* Applid Science, 2019. **9**(21).
4. Sjöström, J., *Chromium Martensitic Hot-Work Tool Steels : Damage, Performance And Microstructure.* 2004.
5. Sam Joshy, A.A., Akshay V.M, Allen M. Chandy, Bharat Nai, *Influence Of Die Temperature On Die Stress Analysis Using Deform 3d.* International Journal Of Mechatronics and Manufacturing Technology, 2020. **5**(1): P. 14-30.
6. Ayer, Ö., *Simulation Of Helical Gear Forming of Az31 Magnesium Material.* Advances In Science And Technology Research Journal, 2017. 11(2): P. 187-191.
7. B.-A. Behrens, T.H., *Numerical And Experimental Investigations on the Fatigue Life of Hot Work Tool Steel X38crmov5-3 Under Forging Process Conditions.* Xii International Conference On Computational Plasticity. Fundamentals And Applications, 2013.
8. Brucelle, O. And G. Bernhart, *Methodology For Service Life Increase of Hot Forging Tools.* Journal of Materials Processing Technology, 1999. **87**(1): P. 237-246.
9. Behrens, B., Et Al., *Numerical Investigations on Stresses and Temperature Development of Tool Dies During Hot Forging.* Key Engineering Materials, 2022. **926**: P. 559-568.
10. Kim, Y.-J. And C.-H. Choi, *A Study On Life Estimation of Hot Forging Die.* International Journal of Precision Engineering And Manufacturing, 2009. **10**: P. 105-113.
11. Gh. Seyed Bagheri1, A., M. Reza Soleymani Yazdi,B, M. Tahmaseb, *Investigation of Forging Process Parameters Effects on Die Fatigue Life Using Numerical Methods.* Applied Mechanics And Materials, 2011. 80-81: P. 937-941.
12. *Shravan Kumar, Crack Propagation, Break Area Microstructure Study on D6 Material Used For Lug Forging Di.* International Journal Of Recent Scientific Research, 2017. **8**(11): P. 1697-21700.

13. Calvo-García, E., *An Experimental Analysis of The High-Cycle Fatigue Fracture of H13 Hot Forging Tool Steels*. Materials, 2022. **15**, Doi: 10.3390/Ma15217411.
14. Shangwira, *Forging Optimisation Process Using Numerical Simulation And Taguchi Method.* Sn Applied Sciences, 2020.
15. Om Prakash Kumar1, V., *Optimization of The Process Parameters of Forging of PitmanArm.* International Journal Of Engineering Science Invention (Ijesi), 2019. **8**(08): P. 01-11.
16. Kumar Satyam, Saurabh Kumar, Rajkumar Ohdar, *Parametric Optimization of Hot Forging Process: A Six Sigma Based Approach.* Edp Sciences, 2021. **309**.
17. Ohdar, R.K., I. Equbal, and V. Kumar, *Die Stress Optimization Using Finite Element And Taguchi Method.* Materials Science Forum, 2013. **762**: P. 319-324.
18. Turki Diwan Hussein1, A., Rasha Abed Alkhider Abed Allah, and Kamil Jaw, *Optimization Of Hot Forging Process By Smart Design And Numerical Analysis Method.* Aip Conference Proceedings 2213, 02021, 2020.
19. Akshay S Nandalgaonkar1, S.C.B., *Design and Analysis of Forging Die Towards Improving Life Of Closed Die By Using Finite Element Analysis.* Ijariie, 2021. **7**(2).
20. Jolgaf, M., Et Al., *Closed Die Forging Geometrical Parameters Optimization For Al-Mmc.* American Journal Of Engineering And Applied Sciences, 2008. **1**.
21. Saleh, M., *The Review Study of Forging And Effects on The Produced Part.* Journal of Mechanical Research And Application 2017. **9**(2): P. 1-7.
22. Sheth, D., Et Al., *Exploring Forging Load In Closed-Die Forging*. 2014.
23. Taylan Altan, G.N., Gangshu Shen, *Cold And Hot Forgings: Fundamentals And Applications.* Asm International, 2005
24. Palumbo, G., *Thermomechanical Processing of Metallic Materials*. 1997, Google Patents.
25. W. Tetlow, R.P.T., *Modelling Of The Effects Of Friction On BulkDeformation Behaviour During Drop-Forging Of AA7075.* International Journal Of Advanced Engineering And Management Research, 2021. **6**(05): P. 37-50.
26. *Metal-Forming-Module-Ii.*
27. Hosford, W. And R. Caddell, *Metal Forming: Mechanics And Metallurgy*. 2011.

28. *The Welding Engineers Guide To Fracture And Fatigue*, P. Moore And G. Booth, Editors. 2015, Woodhead Publishing: Oxford. P. 197-206.
29. T., D.A.U.D., *Metal Forming Handbook*. 1998, Verlag Berlin Heidelberg: Schuler (C) Springer.
30. Božić, Ž., M. Mlikota, And S. Schmauder, *Application of The ΔK, ΔJ And ΔCTOD Parameters In Fatigue Crack Growth Modelling.* Tehnicki Vjesnik, 2011. **18**: P. 459-466.
31. Saleh, M.H., *The Review Study of Forging And Effects On The Produced Part.* Mechanical Research And Application, 2017. **9**: P. 1-7.
32. Shailendra Dwivedi1, G.A.K.K.P., *Modelling of Metal Forming Process For Simulation Process.* Engineering Research And Development (Ijmperd), 2013. **3**(2): P. 181-186.
33. Subramanian, T.L. And T. Altan, *A Practical Method For Estimating Forging Loads With The Use of A Programmable Calculator*. Journal of Applied Metalworking, 1980. **1**(2): P. 60-68.
34. Lukács, Z. And G. Gál. *Numerical Modelling Of Hot Forming And Heat-Treatment Of Annular Gears*. 2012.
35. Gardner, J.D.V., Athulan; Dornfeld, David A *Comparative Study Of Finite Element Simulation Software.* Uc Berkeley: Laboratory For Manufacturing And Sustainability, 2005.
36. Keshtiban, P., A. Taher, And M. Keshtiban, *Practical Study And Finite Element Simulation Of Production Process of The Bush of Gearbox of Mercedes-Benz 10-Wheel Truck By Closed Die Forging.* 2021.
37. Ahmed Dagne Temesgen, M.I.,Bhuvnesh Bhardwa, *Improvement of Hot Forging Process By Minimized Die Stress Using Finite Element Method.* International Journal of Science, Engineering And Technology, 2015. **3**(5).
38. Kumar, V., *Taguchi Method Experimental Design Technique.* International Conference on Science,Technology And Management(Icstm), 2020.
39. Reddy, B.Y.K. And R.G. Brioso. *Automated And Generic Finite Element Analysis For Industrial Robot Design*. 2011.

40. Kawamoto, M.N., Takao, *Statistical Representation Of S-N Curve On The Fatigue Test Results.* Memoirs Of The Faculty Of Engineering, Kyoto University, 1956. **18**(1): P. 30-43.

41. Ceyhanli, U.T. And M. Bozca, *Experimental And Numerical Analysis of The Static Strength And Fatigue Life Reliability Of Parabolic Leaf Springs In Heavy Commercial Trucks.* Advances In Mechanical Engineering, 2014. **12**(7): P. 1687814020941956.

Appendices

Appendix A

A: 1.1. triple crank press PK-300/100 forging machine during forging operation for lower pickaxe piercing die

A: 1.2 cracked lower pickaxe piercing die

A: 1.3 upper die (punch) used for piercing (indenting) operation for making hole.

A: 1.4 the forged hot pickaxe at the moment of end forging operation

A: 1.5 trimmed and semi-finished pickaxes

A: 1.6 finished pickaxe and the shape modified using hammering machine.